Spring 2020

Smart Distributed Generation System Event Classification using Recurrent Neural Network-based Long Short-term Memory

Shuva Das

SMART DISTRIBUTED GENERATION SYSTEM EVENT CLASSIFICATION USING RECURRENT NEURAL NETWORK-BASED LONG SHORT-TERM MEMORY

by

SHUVA DAS

(Under the Direction of Rami J. Haddad)

ABSTRACT

High penetration of distributed generation (DG) sources into a decentralized power system causes several disturbances, making the monitoring and operation control of the system complicated. Moreover, because of being passive, modern DG systems are unable to detect and inform about these disturbances related to power quality in an intelligent approach. This paper proposed an intelligent and novel technique, capable of making real-time decisions on the occurrence of different DG events such as islanding, capacitor switching, unsymmetrical faults, load switching, and loss of parallel feeder and distinguishing these events from the normal mode of operation. This event classification technique was designed to diagnose the distinctive pattern of the time-domain signal representing a measured electrical parameter, like the voltage, at DG point of common coupling (PCC) during such events. Then different power system events were classified into their root causes using long short-term memory (LSTM), which is a deep learning algorithm for time sequence to label classification. A total of 1100 events showcasing islanding, faults, and other DG events were generated based on the model of a smart distributed generation system using a MATLAB/Simulink environment. Classifier performance was calculated using 5-fold cross-validation. The genetic algorithm (GA) was used to determine the optimum value

of classification hyper-parameters and the best combination of features. The simulation results indicated that the events were classified with high precision and specificity with ten cycles of occurrences while achieving a 99.17% validation accuracy. The performance of the proposed classification technique does not degrade with the presence of noise in test data, multiple DG sources in the model, and inclusion of motor starting event in training samples.

INDEX WORDS: Deep learning, Distributed generation system, Genetic algorithm, Islanding detection, Long short-term memory, Multi-class event classification, Optimal feature selection, Smart grid

SMART DISTRIBUTED GENERATION SYSTEM EVENT CLASSIFICATION USING RECURRENT NEURAL NETWORK-BASED LONG SHORT-TERM MEMORY

by

SHUVA DAS

B.Sc., Chittagong University of Engineering and Technology, Bangladesh, 2017

A Thesis Submitted to the Graduate Faculty of Georgia Southern University in Partial Fulfillment of the Requirements for the Degree

MASTER OF SCIENCE

SMART DISTRIBUTED GENERATION SYSTEM EVENT CLASSIFICATION USING RECURRENT NEURAL NETWORK-BASED LONG SHORT-TERM MEMORY

by

SHUVA DAS

Major Professor:	Rami J. Haddad
Committee:	Adel El-Shahat
	Mohammad Ahad

Electronic Version Approved:
May 2020

DEDICATION

This thesis is dedicated to my mom, Sukla Das, and my father, Haradhan Das.

ACKNOWLEDGMENTS

I want to appreciate the support, motivation, and insights that I got from my advisor, Dr. Rami J. Haddad, through my research. In addition to that, I would like to convey my gratitude to the contribution of Dr. Adel El-Shahat and to the support of other faculty members and staff of the Electrical and Computer Engineering Department in my journey to pursue the MS degree. Finally, I am grateful to my parents and my sister for always being there for me and their never-ending support.

TABLE OF CONTENTS

Page

LIST OF TABLES

Page

LIST OF FIGURES

Page

CHAPTER 1

INTRODUCTION

The traditional electrical power grid poses technological and operational challenges because it is centralized with bulk generation sites and long-distance power transmission networks. Moreover, transmission line faults that occur due to events, such as falling trees, can cause a series of failures that may lead the system to significant blackouts (Guha, Haddad, and Kalaani 2015c). Also, the ever-increasing demand for customized, green, and high-quality power supplies has driven the existing generation and transmission system to operate close to an exhaustive limit. In this case, the transmission and distribution losses have also been increased by considerable amounts (Haddad et al. 2018). The rigid constraints for installation of new transmission lines (Bari and Jawale 2016), the environmental impact of conventional power generation using fossil-fuel (Basak et al. 2012), and the traditional steady deregulation process of the electricity market (Georgilakis and Hatziargyriou 2013) have played a vital role in increasing the interest in distributed generation (DG) resources. Moreover, most of these DG resources are photovoltaic (PV) systems, wind energy conversion systems, and fuel cells (Feng et al. 2018), which are renewable and environment-friendly. DGs are generally owned by individuals, industries, or an independent power producer, since DG sources, in general, are cost-effective, emission-free, and resilient (Agency 2018). DGs also contribute to grid reinforcement, reduction in power losses and on-peak operational expenses, and an increase in grid efficiency and reliability (Basak et al. 2012). A DG system is comprised of small-scale (few kilowatts to megawatts) decentralized generating units, which are quiet, compact, and independent (Järventausta et al. 2010). In the US, more than 12 million DG units have been installed under variable policies and incentives, which constitute one-sixth of the total existing centralized generation capacity (Agency 2018).

Generally, DGs are built within the infrastructure of a conventional power system

where centralized control is applied to the transmission system and passive control system to the distribution system ('fit and forgot' approach) (Keane et al. 2013; Boehme, Harrison, and Wallace 2010). Since this approach limits the DG penetration (EURELECTRIC 2013), high penetration of DGs along with active components such as storage devices, dynamic loads, and plug-in hybrid vehicles increase the complexity of grid management. Some major issues that accompany high penetration of DGs are voltage and frequency destabilization, power quality (PQ) variations (Khamis et al. 2013), and protection failure such as out-of-phase reclosing due to relay malfunctioning.

1.1 Islanding Detection

One of the major concerns since the early '80s in DG interconnection is due to increased DG penetration is unintentional islanding (Arritt and Dugan 2015). Islanding occurs when electrical isolation of DGs from the remainder of the power grid occurs. A DG system in islanded mode has been shown in Fig. 1.1.

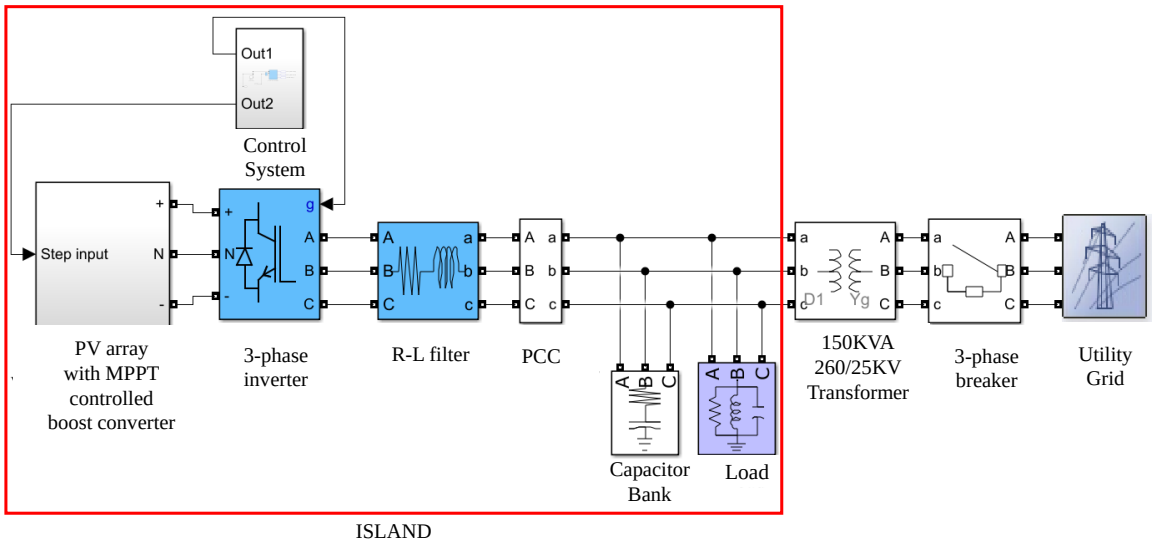

Figure 1.1: Distributed Generation System in islanded mode

A DG system can be designed to offset the demand when the cost of generation is

high by operating in an intentional islanded mode. This way, not only customers benefit financially, but also suppliers can reduce the generation and distribution upgrading costs (OpenEi 2018). However, the problem occurs when DG goes into islanded mode unintentionally due to the malfunctioning of protection equipment, faults, or substation failure. The situation becomes more severe when an isolated subsystem continues to be energized by a DG, and islanding remains undetected by the DG protection system. An islanded DG system can face some significant implications such as reconnection of the islanded system to the grid due to out-of-phase reclosing—DG voltage, and when isolated, it can remain unsynchronized with the grid in islanded mode. So, the reclosing of two systems without protection system coordination in such a situation can feed high currents and torque into the rest of the grid. Moreover, the safety of line workers and field engineers is compromised.

There are several standards (Std.), such as IEEE Std. 1547 (IEEE1547 2003), UL 1741 (UL1741 2001), and IEC 62116 (IEC62116 2008), which mandated detection and control requirements to design Islanding Detection (ID) techniques. IEEE Std. 1547 provided requirement for interconnecting DG resources and grid utility, while UL 1741 set standards for safety measurements of the charge controller and power converter in PV storage systems. IEC 62116 has given test benchmarks for utility connected PV inverters. The maximum islanding detection time set by these standards is 2 seconds. Since the performance of islanding detection techniques can be affected by any change in load quality factor Q_f (ratio of reactive and real power provided by DG source), the standards mentioned above set a constant value (1 or 2.5) for Q_f to be maintained in the system for better detection accuracy. The performance of ID techniques is evaluated using detection time, detection accuracy, and non-detection zone (NDZ) (Li et al. 2019). NDZ is defined as the region of active and reactive power mismatch where islanding remains undetected by an ID technique.

A significant amount of research has been carried over the years to develop ID techniques and their modification. ID techniques based on monitoring and scrutinizing the local parameters, i.e., voltage, frequency, rate of change of frequency (ROCOF), and current at the point of common coupling (PCC) have been categorized into four different classes by the taxonomy (Guha, Haddad, and Kalaani 2015c): active, passive, remote, and machine learning-based techniques as presented in Fig. 1.2.

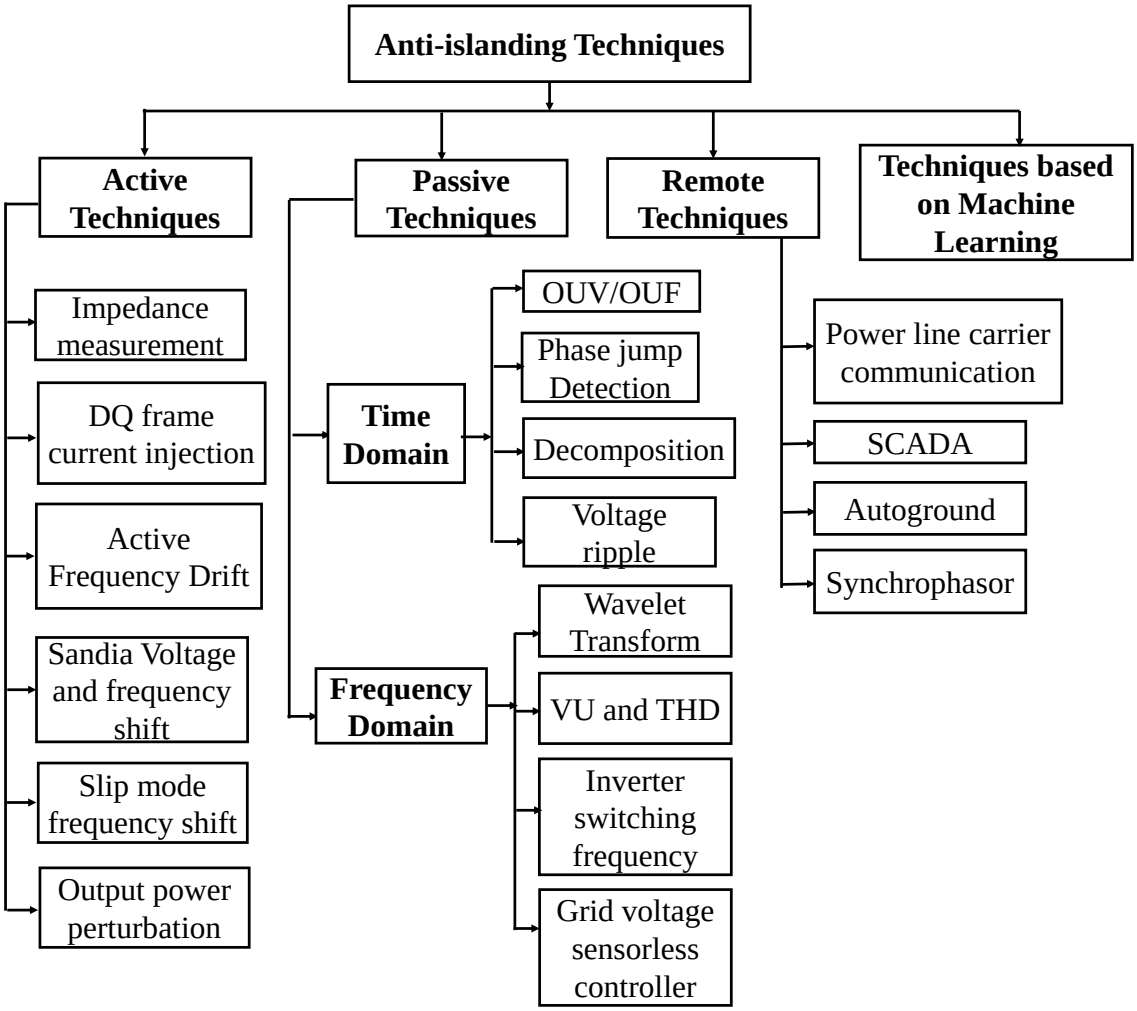

Figure 1.2: Taxonomy of Islanding detection techniques

Active ID techniques analyze the deviation of the local parameters because of intentional disturbances injection after the occurrence of islanding in the DG system. These

techniques are commonly based on impedance measurement (Asiminoaei et al. 2005; Gao, Wang, and Yun 2019; Wen et al. 2016), DQ frame current injection (Gupta, Bhatia, and Jain 2015; Voglitsis, Papanikolaou, and Kyritsis 2019; Murugesan and Murali 2019a), active frequency drift (Kim and Kim 2019; Ropp, Begovic, and Rohatgi 1999; Yafaoui, Wu, and Kouro 2012), Sandia voltage and frequency shift (Vahedi and Karrari 2013; Khodaparastan et al. 2017), slip mode frequency shift (Akhlaghi, Ghadimi, and Akhlaghi 2014) and output power perturbation (Chen et al. 2019; Chen and Li 2016; Park, Kwon, and Choi 2019; Sun et al. 2017). Though active ID techniques offer small NDZ and faster operation than passive ID techniques, they lead to PQ deterioration due to the disturbance fed into the system's control module. On the contrary, passive techniques track and compare the deviation trend of the local parameters monitored at PCC from their predefined threshold value after islanding occurs. These techniques can be divided into two categories based on the approach: time-domain (Raza et al. 2017; Saleh et al. 2016; Guha, Haddad, and Kalaani 2015a; Y. M. Makwana and Bhalja 2017; Guha, Haddad, and Kalaani 2016; Rostami et al. 2019; Ganivada and Jena 2019; Jinsong et al. 2018; Makwana, Bhalja, and Gokaraju 2019; Mlakic, Baghaee, and Nikolovski 2019a; Ruchita et al. 2018; Mohanty et al. 2019; Niaki and Afsharnia 2014) and frequency domain (Das and Chattopadhyay 2018; Muda and Jena 2018; Y. M. Makwana and Bhalja 2019; Dubey, Popov, and Samantaray 2019; Reigosa et al. 2017; Guha, Haddad, and Kalaani 2015b; Samui and Samantaray 2013; Santoso et al. 2000; Hsieh, Lin, and Huang 2008). Time-domain approaches are based on over/under voltage (OUV), over/under frequency (OUF), phase jump detection, decomposition techniques, and voltage ripple detection. On the other hand, the frequency domain approaches are based on wavelet transformation, voltage unbalance (VU), time-harmonic distortion (THD), inverter switching frequency, and grid voltage sensorless controller. Passive ID techniques are cost-effective and technology-neutral, but they often suffer from a larger NDZ margin than active ID techniques and inconvenient tripping. Remote ID

techniques are based on the continuous monitoring system by communication between utility and DG sources using power-line carrier communication (Ropp et al. 2000; Xu et al. 2007; Wang et al. 2007), SCADA (Ward and Michael 2002), autoground (Chad, Brissette, and Philippe 2014), and synchrophasor, i.e., phase measurement (Pena et al. 2013; Sykes et al. 2007). Of some other most recently developed techniques, signal-processing based ID techniques offer a solution to the problem of both NDZ and PQ disturbances. Some advanced signal processing tools for islanding detection are mathematical morphology (Farhan and K 2017), duffing oscillator (Vahedi, Gharehpetian, and Karrari 2012), and S-transform (Ray, Kishor, and Mohanty 2010). These techniques also have shortcomings associated with the level of signal to be decomposed, noise sensitivity, and high computational complexity. Hybrid techniques (Siddiqui, Fozdar, and K. 2017; Murugesan and Murali 2019b; Mlakic, Baghaee, and Nikolovski 2019b; Murugesan, Murali, and Daniel 2018; Kermany et al. 2017; Khodaparastan et al. 2017; Azim et al. 2017) are some of the most recent developments in the field of ID techniques, which are the integration of active and passive ID techniques. However, these techniques incorporate more parameters than other ID schemes to address PQ problems such as frequency deflection, voltage sag, swell, harmonics, and power factor fluctuation.

1.2 Intelligent Approach for Islanding Detection

In the DG system, different non-islanding events are capacitor switching, short-circuit faults, load switching, loss of parallel feeder (LOPF), and a motor starting that can be detected as islanding erroneously. Moreover, the growing system complexity of DGs due to ongoing trends, like smart grids, are urging the development of ID techniques that can process large datasets more efficiently and accurately. The exploitation of smart event classification techniques based on artificial intelligence and machine learning can help DGs to incorporate islanding and different non-islanding scenarios more accurately while as-

suring smart maintenance of overall system stability. The first step of an event classifier's implementation is to design a monitoring and data acquisition system for recording the disturbances in the DG system. Then, these data need to be processed so that features from the selected parameters can be extracted. Finally, extracted features are used to differentiate and classify different DG events. A typical structure of such classification techniques followed in the literature is illustrated below in Fig. 1.3:

Figure 1.3: A typical structure followed in existing event classification techniques

1.3 Summary of Contributions

In this work, the proposed classification technique does not require any complex calculation for feature extraction and is capable of adding intelligence into a DG system in a decentralized fashion. By monitoring some parameter values having certain combinations for different DG events such as islanding, non-islanding, and normal operation mode, this technique logs those parameters. Then, it uses them to classify these events with high accuracy, efficiency, and reliability. Five-fold cross-validation has been used to evaluate the performance validity of the proposed technique. A genetic optimization algorithm (GA) has been integrated with the proposed model to optimize the classifier performance. The optimum numbers of training parameters and the best combination of features selected by GA are applied to the model to analyze for overall classification performance. Finally, the robustness of this technique is validated by testing the trained network's performance for a single DG system under the bulk amount of unseen dataset, noisy dataset, starting of an induction motor in both single DG, and multiple DG system.

The remainder of this thesis is organized as follows. Chapter 2 discusses the different techniques used for the event classification of DG systems. Chapter 3 explains the hypothesis behind choosing the parameters for the detection of different events, the theory behind the proposed technique used for classifying those events based on the time sequence trend of the parameters selected. Chapter 4 presents the simulation of the DG system by integrating photovoltaic sources with the utility grid. Chapter 5 presents the detail about the dataset preparation along with a brief outline of designing the LSTM model used to classify the data and its optimization. Chapter 6 presents the experimental results and findings of this study. Finally, Chapter 7 concludes the thesis with a summary of the proposed DG event classification method and findings.

CHAPTER 2

LITERATURE REVIEW

Mostly, time-domain signal waveforms of voltage and current are used in classification methods presented in the literature. Features that represent unique characteristics of different DG events are extracted using different techniques as per requirements for classification layer input. Table 2.1 summarizes the most recent literature that developed different classification techniques for the DG system, including the feature extraction method and overall classification accuracy. Some commonly used feature extraction techniques in different literature are: Hilbert transform (Chakravorti, Patnaik, and Dash 2018), Slantlet transform (Ahmadipour et al. 2019; Ahmadipour, Borbad M., and Hizam 2019), wavelet transform (Ahmadipour et al. 2019; Khokhar et al. 2017; Eristi et al. 2013; Wang, Ravishankar, and Phung 2019; Kong et al. 2018; Manikonda and Gaonkar 2019), S-transform (Menezes et al. 2019; Ray, Mohanty, and Kishor 2013), Hilbert-Huang transform (Mishra and Rout 2018), morphological filtering (Chakravorti, Patnaik, and Dash 2018; Mishra, Panigrahi, and Rout 2019), etc. The feature extraction technique can be a key factor in the overall performance of the classifier. Different types of DG event cases were classified as: low and high impedance faults, load switching, capacitor switching, DG outage in two different modes: grid-connected and islanded (Mishra, Panigrahi, and Rout 2019). They have used a very new classification technique called extreme learning machine (ELM) with mathematical morphological filtering as the feature extraction method, which achieved an overall classification accuracy of 97.45% and 98.67% for grid-connected and islanded mode respectively. With the same system and classifier, but the Hilbert-Huang transform method as feature extraction (Mishra and Rout 2018), their overall classification accuracy decreased down to 96.99% and 96.75% for grid-connected and islanded mode respectively.

Features extracted using different techniques were used as input of the classifier based

Table 2.1: Comparison of existing DG event classification techniques

References	**Feature Extraction**	**Classifier**	**Accuracy**
(Chakravorti, Patnaik, and Dash 2018)	Hilbert Transform Morphological Filtering	DT DT	99.05% 99.70 %
(Ahmadipour et al. 2019)	Slantlet Transform Wavelet Transform	RPNN	100% 93.33%
(Ahmadipour, Borbad M., and Hizam 2019)	Slantlet Transform	PNN	97.39%
(Khokhar et al. 2017)	Wavelet Transform	PNN	99.875%
(Eristi et al. 2013)	Wavelet Transform	LS-SVM	98.84%
(Wang, Ravishankar, and Phung 2019)	Wavelet Transform	SVM KNN	99.5% 100%
(Kong et al. 2018)	Wavelet Transform	Deep Learning	98.3%
(Manikonda and Gaonkar 2019)	Wavelet Transform	CNN	98.73%
(Menezes et al. 2019)	S-Transform	ANN	99.86%
(Mishra, Panigrahi, and Rout 2019)	Morphological Filtering	ELM	98.67%
(Chandak et al. 2018)	Differential Evolution	K-ELM	99.73%
(Haddad et al. 2018)	PCC Signals	ANN	96.21%
(Baghaee et al. 2019a, 2019b)	PCC Signals	SVM	100%
(Haoran et al. 2019)	PCC Signals	Logistic Regression	100%

on: decision tree (DT) (Chakravorti, Patnaik, and Dash 2018), kernel-based extreme learning machine (K-ELM) (Chandak et al. 2018), artificial Neural Network (ANN) (Menezes et al. 2019; Kumar and Bhowmik 2018; Haddad et al. 2018), relevance vector machine (RVM) (Y. Makwana and Bhalja 2016), support-vector machine (SVM) (Wang, Ravishankar, and Phung 2019; Ray, Mohanty, and Kishor 2013; Baghaee et al. 2019a, 2019b), least-squared support vector machine (LS-SVM) (Eristi et al. 2013; Ray, Mohanty, and Kishor 2013), k-nearest neighbor (KNN) (Wang, Ravishankar, and Phung 2019), and probabilistic neural network (PNN) (Ahmadipour, Borbad M., and Hizam 2019; Khokhar et al. 2017), modular probabilistic neural network (MPNN) (Ray, Mohanty, and Kishor 2013), logistic regression (Haoran et al. 2019), Naive-Bayes classifier (NBC) (Mishra and Rout 2018), etc. A review of the classifiers and a detailed comparison of ID techniques based on these classifiers are presented in this chapter.

2.1 Decision Tree

Decision tree (DT) algorithms use a flowchart to break down a sophisticated model of sequences into some simple sequences by evaluating the possible consequences of the input variable. After comparing the input variable to a specific threshold at each node of decision, the model predicts an event's chance of occurrence. In general, in the beginning, the root node is split into two child nodes based on the defined threshold. Child nodes are then split into different branches until the final 'nodes' called 'leaf' have been found, which represent distinct classes. For islanding detection, DT algorithms search for innate relationships in data sequence and find the distinct characteristics of islanding event cases from other non-islanding event cases.

A decision tree algorithm (Madani et al. 2012) was proposed for islanding detection based on a binary classification method. This study has used an adaptive boosting technique to reduce the rate of classification error. The algorithm was designed with three child

nodes and five leaf nodes. This method gave 100% accurate results in classifying islanding cases with negligible NDZ. Another DT algorithm (Sun, Wu, and Centeno 2011) has been proposed for islanding detection based on data-mining software called 'CART.' Their test on a large-scale power system model had 98% average prediction accuracy. Another decision tree method has been proposed based on the 'Iterative Dichotomiser 3 (ID3)' algorithm (Chandak et al. 2018). In this method, changes in some parameters during islanding and different non-islanding events were plotted graphically. Then, classification is done based on the sensitivity of the parameters for all events considered.

In another literature (Chakravorti, Patnaik, and Dash 2018), another decision tree algorithm was proposed based on fuzzy logic called 'fuzzy judgment tree' to design a multiclass classifier. Two different feature extraction methods were used based on signal processing: multi-scale morphological gradient (MSMG) filter and short-time modified Hilbert transform (STMHT). The proposed classifier was able to classify islanding and different other PQ disturbances with 93.1% and 93.7% accuracy using MSMG and STMHT as feature extraction methods, respectively.

2.2 Artificial Neural Network

Artificial Neural Networks (ANN) replicate the human brain's biological nervous system to process input information for applications such as pattern recognition, forecasting, and curve fitting. ANN is designed with hidden layers called 'neurons' consisting of nodes through which input data is processed with learned weights and bias values and finally sent to the output layer. Activation functions are used to relate between all layer outputs and inputs. Training algorithms control the learning process by which weights are updated through the layers. The number of hidden layers is chosen independently. But ANN models can become complicated with a higher number of hidden layers even though it ensures better performance overall. Feed-forward ANN is mostly used to address power system

problems such as voltage fluctuations, system stability analysis, and fault detection.

Some researches used ANN for addressing islanding detection issues in recent years. A feed-forward ANN model with four passive inputs (Laghari et al. 2014) was proposed for classifying islanding events and non-islanding events. 'Levenberg Marquardt Back Propagation' algorithm has been used for the training process to achieve less training time and reduce the epoch number. The zero NDZ has been achieved with 100% classification accuracy. A similar algorithm was also used for islanding detection (Menezes, Coury, and Fernandes 2019), where the 'Minimal redundancy maximal relevance' method for feature extraction was used to exclude the input parameters with low redundancy. Different types of faults, load switching events, and islanding events were classified with 99.998% accuracy. Another model with ANN was proposed to classify scenarios such as power mismatch, over-voltage, and under-voltage in various power factor conditions (Mehang, Riawan, and B. Putri 2018). In this study, the PCC's voltage has been taken as an input parameter for the ANN training model. Classification Accuracy of 94% has been achieved with a detection time ranging from 0.14s to 0.24s by the model.

A novel classification technique based on ANN was proposed. It incorporated separate ANNs for each parameter (that are readily available at PCC) and used the majority vote fusion algorithm to combine classification outputs of all ANN and generate final classification output (Haddad et al. 2018).

2.3 Support Vector Machine

Support vector machine (SVM) is a popular classification algorithm based on structural risk minimization that can be trained with a smaller dataset with fewer variables. Instead of reducing the dimension, a hyperplane in an ample or infinite-dimensional space is constructed with SVM non-linear mapping. SVM can be handy for classification, regression, or other tasks like outline detection because of these characteristics. In practice,

the SVM algorithm is implemented using a kernel that connects the input vectors named as support vectors to the test vectors. By transforming the problem using some linear algebra, the learning of the hyperplane in linear SVM is done. Moreover, the process of solving the SVM model is by using an optimization procedure. The search for coefficients of the hyperplane is done by using a numerical optimization procedure.

A multi-feature based technique with SVM classifier was proposed to detect islanding (Alam, Muttaqi, and Bouzerdoum 2014). Features were extracted for various power imbalance cases, along with islanding, and then the SVM classifier was trained with both linear and polynomial kernel. With the linear kernel, the islanding detection rate was 99.53%, with a 0% false alarm rate. But with the polynomial kernel, though the detection rate increased to 99.62%, the false alarm rate was increased to 4.13%. A radial bias function was used as the kernel to design the SVM classifier for ID (Matic-Cuka and Kezunovic 2014). Five fold-cross validation method with the bootstrapping method was used for performance evaluation. The classification accuracy achieved for ID was 98.94%, while the overall accuracy was 99.49%, with 0.6277% of uncertainty. SVM was proposed for islanding and grid fault detection and for protection of PV-based microgrids with PHEV (Baghaee et al. 2019a), which will be discussed later in another section in this chapter.

2.4 Probabilistic Neural Network

Probabilistic Neural Network (PNN) has been modeled using a Bayesian technique to use for applications such as pattern recognition. Designing PNN requires four-layers: an input layer, pattern layer, summation layer, and an output layer. Not only the fact that PNN guarantees convergence if given enough data, but also the high speed of the convergence process makes it very much useful as a real-time fault detection technique and signal classifier. A PNN model was proposed to detect islanding (Ahmadipour, Borbad M., and Hizam 2019). The model used a unique feature input vector for training that was decomposed

by ‘Slantlet Transform’ from the PCC signal waveform. The performance of the proposed model was evaluated under different load conditions, and finally, 97.39% of accuracy was achieved. Khokhar et al. proposed a new feature selection algorithm that integrates ‘discrete wavelet transform’ as a feature extraction method and PNN as a classifier for detecting different PQ disturbances in the DG system. A technique called ‘Artificial Bee Colony’ has been used to determine the optimum number of features. 99.875% of accuracy has been achieved after using optimum features for training, which is best reported using PNN.

An improved version of PNN called Ridgelet PNN (RPNN) has been used for islanding detection (Ahmadipour et al. 2019). Both ‘Slantlet transform’ and ‘discrete wavelet transform’ techniques have been used as feature extraction methods with RPNN to classify islanding and other DG events. With ‘Slantlet transform’, 100% accuracy has been achieved, while 93.33% accuracy has been achieved with dataset extracted using ‘discrete wavelet transform’. Another modified version of PNN called modular PNN (MPNN) (Ray, Mohanty, and Kishor 2013) was used to classify different PQ events. S-transform has been used for feature extraction, and SVM and LS-SVM were also used to compare the results. Though MPNN performed better than the other two in the simulated environment, with the experimental setup, LS-SVM outperformed both MPNN and SVM. However, PNN and its modified versions are slower than multi-layer perceptron networks at classifying new cases.

2.5 Logistic Regression

Logistic regression is a supervised machine learning algorithm for binary classification. It uses the logistic function, also called the sigmoid function $\sigma(x) = \frac{1}{1+e^{-x}}$ that can take any real-valued number and map it into a value between 0 and 1. A classification technique based on logistic regression (Haoran et al. 2019) was proposed to classify islanding and non-islanding events. Features with a high correlation have been selected, which

then was followed by the training process under the TensorFlow environment. The trained network performed well on predicting 16 test cases with 100% accuracy.

2.6 Comparative Analysis

Though some of the literature (Khokhar et al. 2017; Eristi et al. 2013; Wang, Ravishankar, and Phung 2019; Ray, Mohanty, and Kishor 2013) classified the system's PQ disturbances with higher accuracy, these techniques were unable to find the root cause of these disturbances. Classification techniques (Chakravorti, Patnaik, and Dash 2018; Ahmadipour et al. 2019; Ahmadipour, Borbad M., and Hizam 2019; Chandak et al. 2018; Kumar and Bhowmik 2018; Y. Makwana and Bhalja 2016; Baghaee et al. 2019a, 2019b; Haoran et al. 2019) classified a wide range of DG events, including islanding with high accuracy and faster detection time. Islanding detection technique, proposed in some literature (Haddad et al. 2018; Baghaee et al. 2019a, 2019b; Haoran et al. 2019), used the available parameter signals at PCC and detected islanding with a high accuracy rate. However, techniques used in some literature (Baghaee et al. 2019a, 2019b) still suffered from 9.52% NDZ. Moreover, few islanding cases were compared to the non-islanding cases for classification used in these studies (Haoran et al. 2019). Moreover, none of these techniques considered the 'normal operation' as an output class, which might otherwise affect the classifier's performance. Since DGs pose the probability of misidentifying an islanding event as a grid-connected mode or vice-versa, exclusion of feature data characterizing the ideal mode of operation as input can improve the overall classification accuracy artificially. Since most of the classification techniques were designed to classify all the DG events in two classes: islanding and non-islanding, they were unable to classify the considered events into root causes. Also, most of these classification techniques were performed over data extracted from the system with conventional sources of generation. The performance of some classifiers (Wang, Ravishankar, and Phung 2019; Chandak et al. 2018), also sig-

nificantly degraded after adding noise to the feature data. However, one study (Haddad et al. 2018) was able to classify different DG events, including the ideal mode of operation, with 96.21% average accuracy. Their proposed classifier was less sensitive and sometimes not accurate while predicting real mismatch scenarios. Moreover, this study investigated the performance of the proposed classifier on the individual occurrence of the events because the probability was getting lower while coinciding with two or more events.

Classification of different DG disturbances to their root cause events can be achieved with accuracy, reliability, and precision in two ways: 1) improving the prediction ability and reducing the dependency on the threshold by optimal selection of more features, 2) using deep learning into the classification model of non-linear data to improve the learning capability of complex data characteristics. There are little research efforts toward incorporating deep learning into a binary classification of islanding, non-islanding events, and normal operation cases. Deep learning uses the multi-layer perceptron network to learn the characterizing pattern of data with multi-level generalization and complex computation, which can improve the accuracy of event classification even if data from two or more events concur. A deep learning framework was proposed (Kong et al. 2018) that used wavelet transform to extract eigenvector representing different DG events (islanding, voltage sag, and swell). Then the eigenvector was passed through stacked auto-encoders for a layer-wise pre-training under three hidden layers. Finally, a supervised fine-tuning process was used to minimize the loss function, and a SoftMax regression layer was used to produce a prediction on a given test set. Though they achieved a higher accuracy of 98.3%, this study did not consider any non-islanding cases in their classification.

Another study proposed a classification technique (Manikonda and Gaonkar 2019) based on a convolutional neural network (CNN), which converted the time-series data of different DG events (islanding, non-islanding, and normal operation mode) into scalogram images using continuous wavelet transform. The scalogram image data set was input

through three convolution layers, each having a filter size of $3\times$ $3\times$ 3, a different number of filters, one rectified linear unit (ReLU) operation, and one max-pooling operation. Finally, one fully connected layer and SoftMax layer has been used to finalize the output. This classifier was designed to classify the input dataset into two output classes: islanding and non-islanding. This classifier was also unable to classify the input data into their root causes. Moreover, transforming the data into an image using a continuous wavelet transform adds excess redundancy and requires intensive computational effort. So, we need to design classifier models that can classify a broad range of islanding and non-islanding events to their root causes not only accurately but also efficiently and reliably. Moreover, such techniques must be able to differentiate between the normal operation mode and different fault events with a low misclassification rate.

CHAPTER 3

PROPOSED METHODOLOGY: TECHNICAL DETAILS

The proposed technique to classify different power system events conforming to their root cause is developed using time sequence to label classification techniques based on LSTM. In this technique, a model with LSTM cells detects the behavior pattern of some predefined parameters over a time period regarding an event. In a distributed generation system, inverter-based DGs produce harmonics due to DC link voltage-ripple, high-frequency switching, and dead time when connected to the grid. These harmonics are controlled using filters and inverter-embedded control techniques to keep them below 5%, according to IEEE std. 1547 (IEEE1547 2003). Events, for example, islanding, unsymmetrical faults, capacitor switching, load switching, and loss of parallel feeder, can contribute to an increase in the magnitude of harmonics in the system. The distinctive pattern of the time-domain signal representing an electrical parameter like voltage at DG point of common coupling (PCC) during such events can be used as a valid index for the detection of islanding and other grid transients. In this section, the hypothesis behind choosing the parameters for the detection of different events, and the theory behind the proposed technique used for classifying those events based on the time sequence trend of the parameters selected are presented.

3.1 HYPOTHESIS

In this study, the parameters taken into account for the proposed classification technique are: voltage in per unit (V_{pu}), rate of change of voltage ($\frac{dV}{dt}$), rate of change of real power ($\frac{dP}{dt}$), power factor (PF), rate of change of power factor ($\frac{dPF}{dt}$), frequency (f), rate of change of frequency ($\frac{df}{dt}$), voltage total harmonic distortion (V_{THD}), and current total harmonic distortion (I_{THD}). These parameters are widely used in different existing islanding

detection techniques (**0**). Signals depicting these parameters also show different behavior during other fault events such as line-to-line (LL), single-line-to-ground (SLG), and three-phase fault (3-ϕ fault). Frequency domain analysis of RMS voltage (V_{RMS}) was done to understand this behavior. From Fig. 3.1, it can be seen that these three events have distinct sub-transient behavior, which leads to a distinct temporal characteristic. Similar behavior was also observed in the case of other parameters mentioned above. So the proposed classification technique was initialized using these parameters as described in chapter 5.

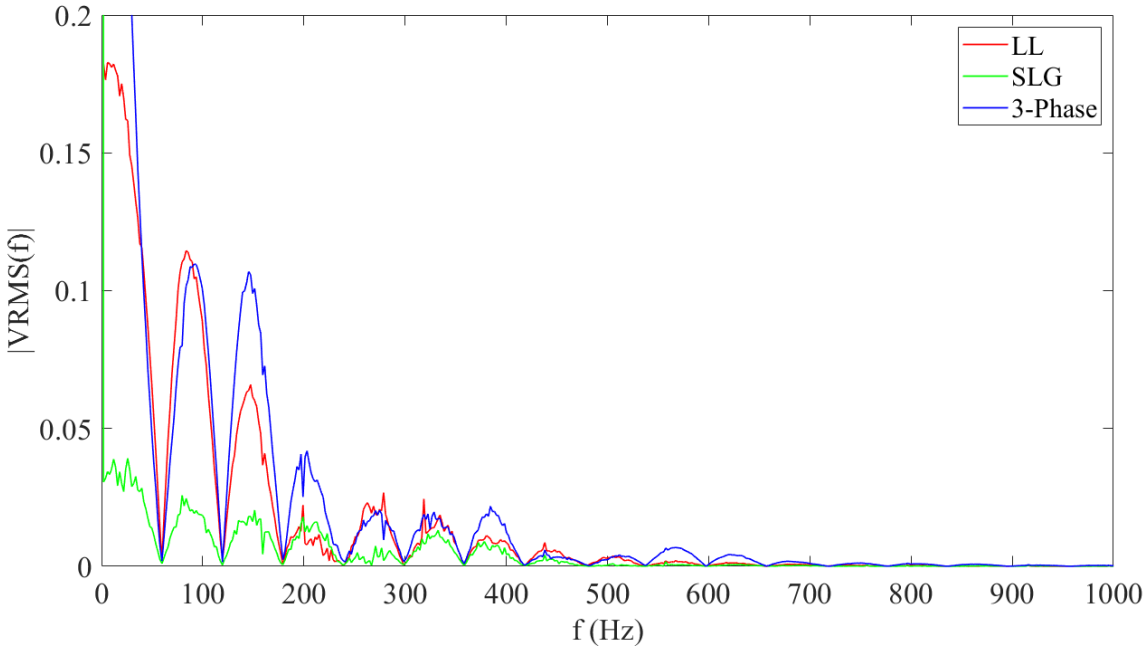

Figure 3.1: Comparison of V_{RMS} for LL, SLG, and 3-ϕ faults in the frequency domain

3.2 Deep Learning for Modeling Time Sequence

Artificial Neural Network (ANN), first introduced in 1943 by McCulloch and Pitts (McCulloch and Walter 1943), has emerged as the most important architecture of deep learning in the last ten years because of the development of a high-speed processing unit. Though ANN works well in learning patterns from large dimensional data by employing multilayer

perceptron, it is not the perfect model to learn the dataset organized in a sequential manner such as time sequence data. Recurrent neural network (RNN) was proposed to solve this problem, which allows connections among hidden units associating a time delay with the same multilayer perceptron architecture. The model can retain past information and establish a temporal correlation between recent input events and present input events. Though Hopfield proposed the early concept of time sequence retention as an associative memory (Hopfield 1982), RRN is developed based on David Rumelhart's work in 1986 (**3**). The basic RNN operation can be formulated as:

$$h^t = \sigma_{sigmoid}([P^y * x^t + Q^y * h^{t-1}] + R) \tag{3.1}$$

$$y^t = h^t \tag{3.2}$$

Where P^y and Q^y are input weight and recurrent weight, respectively, and R is the bias value. σ denotes to gate activation function, x^t denotes the inputs at time t, and h^{t-1} denotes the output of the previous hidden state. y^t is the output of the RNN.

Early attempts on RNN, such as 'Back-Propagation through Time' (Williams and Zipser 1995; Werbos 1988), or 'Real Recurrent Learning' (Robinson and Fallside 1987) often failed due to the 'exploding gradient' and 'vanishing gradient' problems (Hochreiter 1991; Bengio, Boulanger-Lewandowski, and Pascanu 2013). Due to these problems, the scope of RRN to have access to the previous state information becomes limited, which leads to a declination of influence that an input hidden layer has on network output. Therefore, Hochreiter and Schmidhuber proposed a novel and improved version of RNN, Long Short-term Memory (LSTM) (Sepp and Jürgen 1997).

LSTM uses an efficient gradient-based algorithm to learn to connect the time intervals greater than 1000 steps without losing the capability of short-time lag even if the input time sequence is noisy and incompressible. This is done by enforcing the inner states of

hidden units called ‘memory cell unit’ to flow a constant error through them by truncating the gradient computation at a certain point. Each sophisticated LSTM cell unit has the same input and output as normal RRN, while LSTM has three gates in the memory cell to control the flow of information. These gates are called: ’input gate’, ’forget gate’, and ’output gate’, where the ’input gate’ and ’output gate’ are multiplicative. These gates pass the corresponding information through some neural layers of sigmoid function (output is a vector of real numbers from 0 to 1) and point by point multiplication operations (Olah 2015).

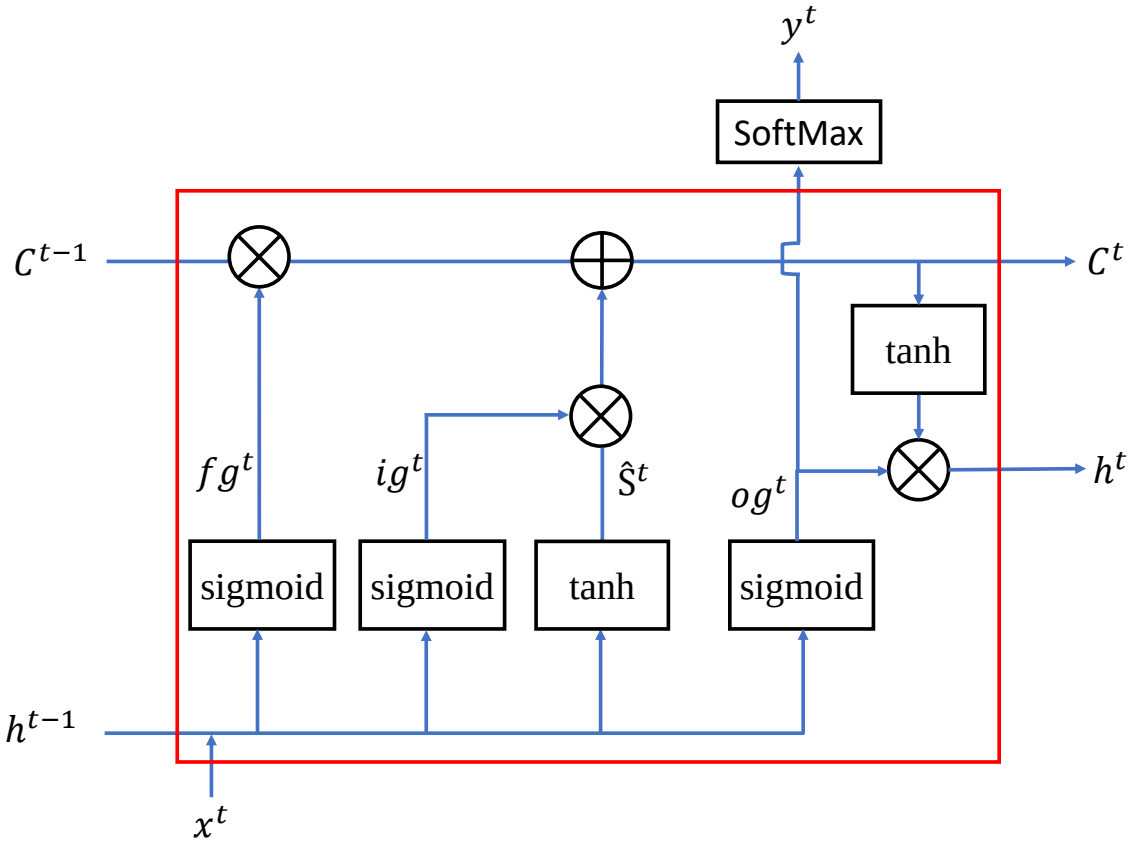

Figure 3.2: Block diagram of LSTM memory cell

The key of LSTM is the cell state of each memory cell unit, as shown in Fig. 3.2, denoted as C^t. At first, LSTM inputs undergo screening to discard some information through

the 'forget gate'. The inputs of the 'forget gate' are previous hidden state, h^{t-1}, and current cell input, x^t. The output of the 'forget gate' is computed with parameters called weight, P^f and Q^f and bias, R^f using equation 3.3 (output is a vector with values between 0 to 1 and the same size as previous cell state C^{t-1}):

$$fg^t = \sigma_{sigmoid}([P^f * x^t + Q^f * h^{t-1}] + R^f) \tag{3.3}$$

Then, the next step is to add selective information to the cell state, which is done using two operations: firstly, the information of previous hidden state, h^{t-1} and current cell input, x^t using weight, P^i and Q^i and bias, R^i are passed through sigmoid operation to get ig^t. Secondly, an output denotes as $\tilde{S}^t$ is computed by using a tanh layer and weight, P^c and Q^c and bias, R^c. Both ig^t and $\tilde{S}^t$ are then combined to create an update on cell's state. These operations are formulated in equation 3.4 and 3.5.

$$ig^t = \sigma_{sigmoid}([P^i * x^t + Q^i * h^{t-1}] + R^i) \tag{3.4}$$

$$\tilde{S}^t = tanh([P^c * x^t + Q^c * h^{t-1}] + R^c) \tag{3.5}$$

Next, the cell state can be updated from C^{t-1} to C^{t-1} by the operation, formulated as equation 3.6.

$$C^t = fg^t * C^{t-1} + \tilde{S}^t * ig^t \tag{3.6}$$

Finally, the 'output gate' computes the updated hidden state output to be sent to the next LSTM cell based on the cell state, but not before some filtering (Olah 2015). At first, the previous hidden state, h^{t-1}, and the current cell input, x^t, are undergone sigmoid operation with parameters, P^o, Q^o, and R^o to output, og^t. Then og^t is multiplied by the manipulated cell state, $tanh(C^t)$ (to get value between -1 to 1). These operations are formulated as:

$$og^t = \sigma_{sigmoid}([P^o * x^t + Q^o * h^{t-1}] + R^o) \tag{3.7}$$

$$h^t = og^t * tanh(C^t) \tag{3.8}$$

Prediction y_t at each time step in LSTM operation is extracted by a SoftMax operation of og^t.

CHAPTER 4

MODELING OF DISTRIBUTED GENERATION SYSTEM

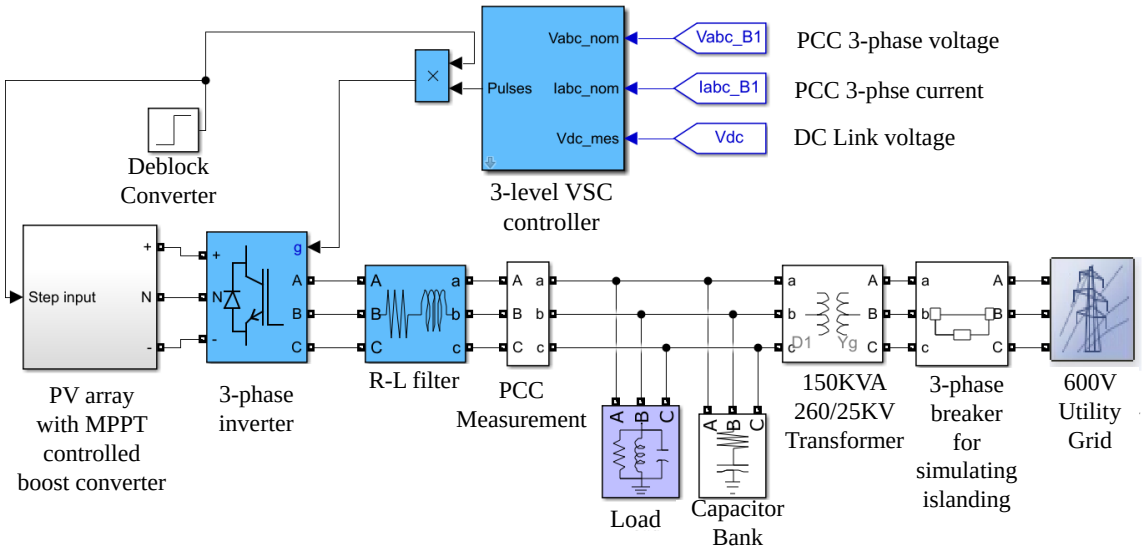

Figure 4.1: Simulation model of PV system connected with grid

A grid-connected photovoltaic (PV) array with a generation capacity of 100.7 kW at standard operating conditions (1000 W/m^2 irradiance and 25° temperature) was designed using the MATLAB Simulink model (Giroux et al., n.d.) as shown in Fig. 4.1:

The PV array was connected to the grid via a 5 kHz DC-DC boost converter operating with a switching duty cycle optimized by a Maximum Power Point Tracker (MPPT) and a three-phase inverter. The MPPT controller was designed based on the 'Incremental Conductance + Integral Regulator' technique (Hasan 2019). This MPPT system automatically varied and optimized the duty cycle to generate the required voltage (500V DC) by increasing the PV natural voltage (273V DC) at maximum power. A three-level, three phases VSC was used to covert the 500V DC link voltage to 260V AC, which had two control loops. The first loop was an external control loop with a DC voltage regulator, which regulated the DC link voltage to +/- 250V to generate I_d reference voltage using a sample time of 100

microseconds. I_q reference was set to zero so that a unity power factor can be maintained. The second loop was an internal loop with a phase-lock loop (PLL) measurement block and a current regulator. PLL measurement block normalized the voltage and current signals at the primary side of the transformer by converting them into park transformed (dq) values and using 100 μsec sample time. The current regulator generated the required V_d and V_q values based on reference I_{dq} values and normalized V_{dq} values. V_d and V_q voltage outputs of the current regulator were normalized into three modulating signals U_{abc} references used by the PWM Generator using 1 microsecond sample time so that an appropriate resolution of PWM waveforms can be achieved. The three-phase inverter was then connected to a utility grid (120kV transmission system and 25kV distribution feeder) having an X/R ratio of 7 and 2500 MVA short-circuit capacity via 100 KVA three-phase coupling transformer (260V/25KV). The 100.7 kW PV array used 330 SunPower modules (SPR-305E-WHT-D), one of the various types of NREL system advisor model. A 10 kVAR capacitor bank was connected to the PCC measurement side to provide reactive support to the load. The model was then modified to simulate different DG events, as listed in Table 4.1.

Table 4.1: Simulated DG event cases for proposed classification technique

Events	**Parameter Range**
Capacitor Closing Events	250-3000 kVAR capacitor
Capacitor Opening Events	250-3000 kVAR capacitor
Line-to-Line Faults	1-60 Ω fault resistance
Load Closing Events	1-100 MVA load
Load Opening Events	1-100 MVA load
Loss of Parallel Feeder	1500-3500 MVA_{sc} infinite bus
Reactive Power Mismatch (islanding)	-10% to +10% mismatch
Real Power Mismatch (islanding)	-50% to +50% mismatch
Single Phase Faults	1-60 Ω fault resistance
Three Phase Faults	1-60 Ω fault resistance
Normal Operation	50% to 150 % DG capacity

CHAPTER 5

PROPOSED DEEP LEARNING MODEL IMPLEMENTATION

Four steps were followed for implementing our proposed DG events classification method: 1) parameter sweeping and feature extraction, 2) data pre-processing, 3) LSTM model construction, and 4) Model Optimization.

5.1 Parameter Sweeping and Feature Extraction

As mentioned earlier, initially, we started with recording nine parameters in total, which follow a distinct pattern trend during ten different DG events along with normal operation mode. Signals depicting these parameter values at PCC for different events were acquired as time-series cells for a simulation run time of 4 seconds and a sampling rate of 0.00001 seconds using MATLAB/Simulink. All of the different DG events were simulated so that they occur at a specific interval (2.5 seconds.) A particular distribution of specific parameters related to those events was followed, as provided in Table 4.1. The specific portion of each parameter value containing the event characteristics in all the cases was extracted as MATLAB data separately from the time series cells.

5.2 Data Pre-processing

In the data pre-processing step, one cell array containing input matrices as time sequences belong to different events, and a categorical array containing output classes was generated. Each input sample in a time sequence denotes the mean over one cycle for a signal representing a specific parameter. For each parameter, ten consecutive cycle means combined, represented a moving window of an input feature to the LSTM. The size of the moving window was selected to feature the most significant effect of a DG event on a spe-

Table 5.1: Organization of time sequence data matrix in the input cell array

$Mean_{11}$	$Mean_{12}$	$Mean_{13}$	...	$Mean_{1M}$
$Mean_{21}$	$Mean_{22}$	$Mean_{23}$	...	$Mean_{2M}$
$Mean_{31}$	$Mean_{32}$	$Mean_{33}$	...	$Mean_{3M}$
...	...	...	...	...
...	...	...	...	...
...	...	...	...	...
$Mean_{k1}$	$Mean_{k2}$	$Mean_{k3}$	...	$Mean_{kM}$

cific parameter. Moreover, it ensured that the classification process was fast enough. In this study, the best performance was achieved by selecting the moving window size as ten by a thorough investigation with a time delay of 166ms. The time delay was reasonable since the IEEE std 1547 (IEEE1547 2003) mandated islanding detection delay limit is 0.2s. Each time sequence has all the parameter values of fixed length as input feature samples for a specific DG event. In the data matrix of a time sequence, as depicted in Table 5.1, any given row represents the moving window of a feature over a ten cycle period. The time series trend of various features is represented in each column. Here, k denotes the total number of features considered to train the classifier, and M represents the size of the moving window. A total of N time sequence matrices, each representing different DG events were combined into cell array as input to the classifier based on LSTM. A categorical array of the same length, as the input cell array, was generated to represent the class number of the sequences.

5.3 Model Construction

In the model construction stage, a classifier was designed for the sequence to label classification based on LSTM concatenating five layers, as shown in Fig. 5.1. The sequence input layer was used to take the sequence data as input to the LSTM network, which is the second layer of the classifier. The sequence input layer sets the size of the input, specified as a vector of positive integers. In this model, the input size was a scaler corresponding to the number of features in the vector sequence input. While passing sequence input to the LSTM network, the input sequence can be padded, truncated, or split to ensure a specified sequence length in each mini-batch. Since the LSTM network can work with inputs having variable sequence lengths, to decrease the amount of padding, input data sequences should be sorted by the sequence length. Since our model has input sequences of a fixed length, there was no need for sorting the input data sequences.

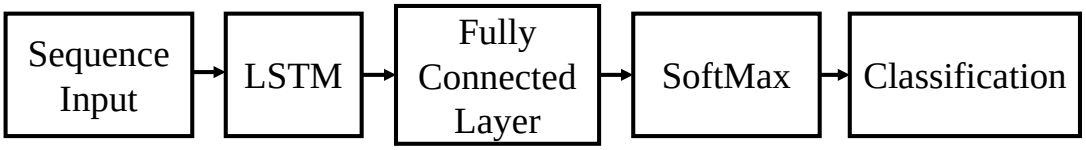

Figure 5.1: Design process of proposed DG event classification

Fig. 5.2 illustrates the flow of time sequence data, x with k features (parameters) of length M through an LSTM layer. Here, h_t and c_t denote the output (also known as a hidden state) and cell state at a time step t, respectively. The first LSTM block produced both the hidden state and the updated cell state using the initial state of the network and the first step of the input sequences. The updated cell state, along with the inputs belonging to the next time step from the input sequence, was used by the next LSTM layer to calculate the hidden state and another updated cell state. For example, at time-step t, LSTM block uses the current cell state (c_{t-1}) and hidden state (h_{t-1}) of the network along with input x_{1t}, x_{2t},..., x_{kt} and produced the hidden state output h_{1t}, h_{2t},..., h_{Nt} containing the output of

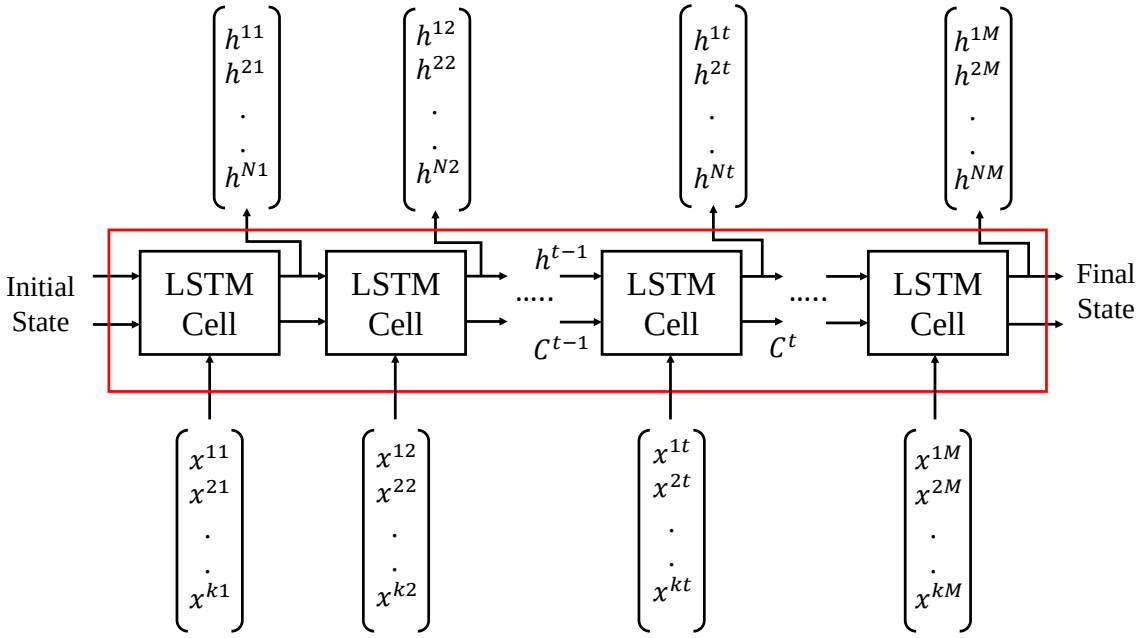

Figure 5.2: Flow of time sequence data through LSTM cells

the LSTM layer for that time step and new cell state c_t containing learned information from the time step t. Here, N is the number of hidden units selected for DG event classification. At each time step, LSTM layers added information to the updated cell state, or removed information from the current cell state using the input gate, forget gate, and output gate, described in section 2.

A fully connected layer then followed the LSTM layer, where all neurons in a fully connected layer were connected to all the neurons in the previous layer. A fully connected layer is basically a multi-layer perceptron that can learn non-linear combinations of the features (the final output of the LSTM layer) in a discriminate manner to identify the object class. This is the reason that the size of a fully connected layer is set as the same as the number of output classes. A SoftMax layer was used to calculate the output of the fully connected layer from its net input. It used the SoftMax function also known as multi-class generalization of logistic sigmoid function (Bishop 2006) to model the class-conditional probability p(x|C_p) and class prior probability, p(C_p) and used them to calculate the poste-

Table 5.2: Training options for classifier

Training Options	**values**
Solver	adam
Execution environment	cpu
Gradient Threshold	1
Sequence length	longest
Shuffle	every-epoch

rior probability p(C_p|x) with Bayes' theorem:

$$p(C_p|x) = \frac{p(x|C_p) * p(C_p)}{\sum_{i=1}^{p} p(x|C_i) * p(C_i)} = \frac{exp(a_p(x))}{\sum_{i=1}^{k} exp(a_i(x))} \tag{5.1}$$

where, a_p=$ln(p(x|C_p) * p(C_p))$. The normalized exponential is the SoftMax function which indicates that if $a_p > a_i$ for all $i \neq p$, then $p(C_p|x) \simeq 1$ and $p(C_i) \simeq 1$.

Finally, a classification layer was used, which took the values from the SoftMax function and assigned each input sequence to one of the K distinct classes. This layer used the cross-entropy function to calculate the cross-entropy loss (as given in equation 10) (Bishop 2006).

$$Loss = \frac{1}{X} * \sum_{1}^{X} \sum_{1}^{Y} t_{xy} * ln(L_{xy}) \tag{5.2}$$

Where, X is the sample number, Y is the total class number, t_{xy} indicates the xth input from yth class. L_{xy} denotes the output label for the xth sequence from the yth class, which is, in another way, the output value from the SoftMax function. So, loss associates the probability of the xth input belonging to the class y.

After the selection of the layers, the training options for the classifier were specified, as listed in Table 5.2. Then the classifier was trained and validated using k-fold cross-validation (Stone 1974). Fig. 5.3 illustrates the concept of 5-fold cross-validation as we

set k=5. Here, the whole dataset was divided into five subsets randomly where each subset contained equal numbers of data from different events. The classifier was trained using four of these subsets, and the performance of the trained classifier was validated using the rest of the subset. After five rounds of cross-validation, the whole process was repeated ten times to validate the classifier's robustness. And then, the average classification accuracy in whole was calculated as a performance index.

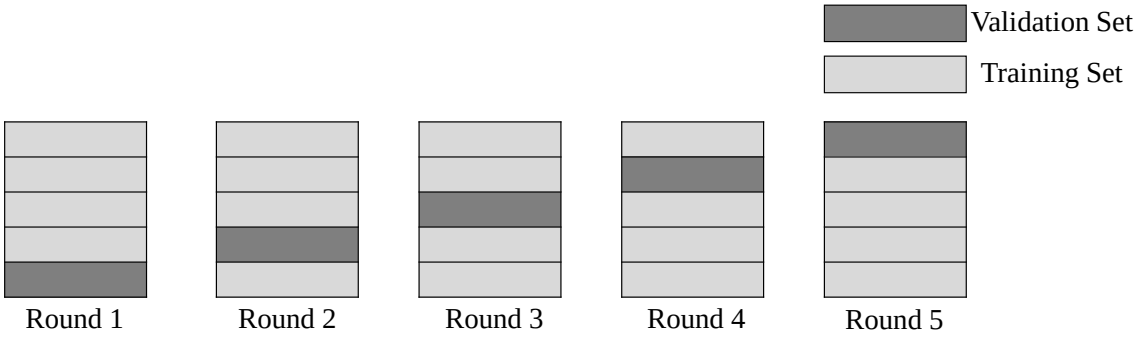

Figure 5.3: Illustration of 5-fold cross-validation concept

5.4 Model Optimization

Though accuracy is a significant function to evaluate the performance of a classifier, reliability and efficiency can be improved with proper selection of training parameters by maximization of objective functions. Four objective functions were considered: accuracy, sensitivity, specificity, and precision. Accuracy goes proportionally with the total number of actual positive (P) and negative (N) cases that are correctly predicted as true by the trained network. Sensitivity measures the proportion of the actual positives (a true positive (TP) and the false-negative (FN)) that are correctly predicted as true by the trained network. In contrast, specificity measures the proportion of actual negatives (true negative (TN) and false positive (FP)) that are predicted as true accurately. Precision measures the proportion

of positive results that are true positive. For instance, high sensitivity on islanding case prediction means few numbers of islanding cases were rejected incorrectly. Similarly, high specificity on islanding case prediction means few numbers of other DG events were mis-predicted as islanding. On the other hand, precision indicates how accurate the classifier was when it predicted an event as islanding. These objective functions were calculated from the confusion matrix for the prediction on unseen test cases using the trained model and formulated (Tom 2006) as equation 5.3-5.6:

$$Accuracy(A) = \frac{TP+TN}{P+N} \tag{5.3}$$

$$Sensitivity(Se) = \frac{TP}{TP+FN} \tag{5.4}$$

$$Specificity(Sp) = \frac{TN}{TN+FP} \tag{5.5}$$

$$Precision(P) = \frac{TP}{TP+FP} \tag{5.6}$$

$$CostFunction(CF) = \frac{\sum_{i=1}^{N}(A)+\sum_{i=1}^{N}(Se)+\sum_{i=1}^{N}(Sp)+\sum_{i=1}^{N}(P)}{N} \tag{5.7}$$

$$Gap = 100 - CF \tag{5.8}$$

The overall performance of the proposed model has been calculated using equation 5.7, where N is the number of events classified. The gap in the overall performance from the desired value, as stated in equation 5.8, can be minimized by integrating a genetic algorithm (GA) into the LSTM network. GA can be used to make a proper selection of hyper-parameters in training options integrating MATLAB optimization toolbox and Deep Learning Toolbox. Moreover, the computational burden can be overcome during feature extraction if the optimum combination of input features can be determined using an optimization algorithm like GA. The flowchart is shown in Fig. 5.4, illustrating the proposed optimized model using GA, is given below:

The process of model optimization consisted of two stages: 1) selection of the optimum number of hidden units, maximum epoch, and mini-batch size, 2) finding the optimal

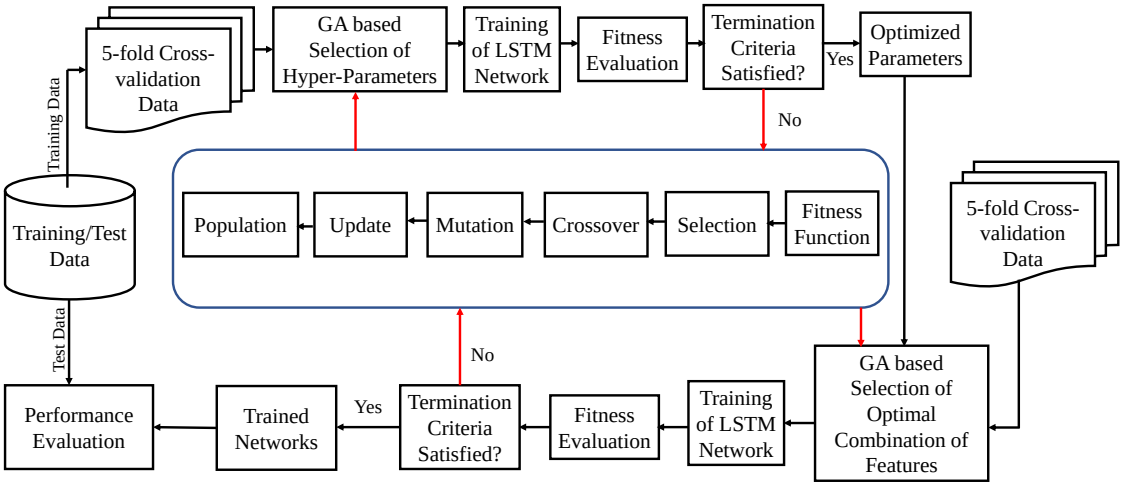

Figure 5.4: Flowchart of GA integrated model for optimum hyper-parameters and the best combination of feature selection

combination of features using the hyperparameters determined from the first stage in the LSTM training. In the first stages, the initial population composed of possible solutions were generated randomly, and chromosomes were encoded in double vector. Then GA started exploring the search space for the superior solution by selection and reproduction operator. The fitness function has been chosen carefully to determine the value of the overall performance value using equation 5.7. The fitness of each chromosome was calculated using equation 5.8. The chromosome returning the smallest fitness value was selected as an optimum solution. When termination criteria were satisfied, GA returns the optimum value of the hidden unit number, maximum epoch number, and mini-batch size, which were used in the second stage, i.e., optimum feature selection. A population size of 50, scattered crossover, and 0.1 mutation rate was selected in this stage. In the second stage, a similar process was repeated, except the chromosomes used in this stage were encoded in binary bits. Where bit 1 represented the selected features for fitness evaluation. A population size of 9, scattered crossover, and 0.1 mutation rate was used in this stage. 30 generations were

used as termination criteria.

CHAPTER 6
SIMULATION RESULTS

A total of 1100 events on the DG model with a single DG source were generated for evaluating the performance of the proposed classifier. As described earlier, GA was applied to investigate optimal hyper-parameter values and the best combination of features for the proposed LSTM model with defined layers and specified training options. The optimal value of hidden units, maximum epochs, and mini-batch size were determined by GA as 108, 70, and 34, respectively. The best combination of features, selected by GA, are listed in Table 6.1.

6.1 Classification results for single-source DG model

Five-fold cross-validation was conducted ten times to evaluate the robustness of the model with these optimal input features. Very high classification accuracy of 99.17% on average was observed with high overall sensitivity, specificity, and precision. Accuracy, sensitivity, specificity, and precision of each event on average are listed in Table 6.2.

Based on Table 6.2, the classification accuracy of each event was above 99.5%. From the sensitivity analysis, it is clear that the proposed technique can identify non-islanding events correctly in more than 98% of cases and islanding events in more than 97% of cases. From the thorough investigation of the confusion matrix of all cross-validation cases, it was seen that this technique was misclassifying the real power mismatch events as reactive power mismatch events or vice-versa. The lower average precision value of reactive power mismatch (98.5%) and real power mismatch (97.55%) than other events is also an indication that the proposed technique may have been confusing these two events. But in overall, the technique was able to differentiate an islanding case from other non-islanding cases with very high overall precision. To justify this issue, all the non-islanding cases,

Table 6.1: Optimal combination of features selected by GA

Name of the Parameters	**Symbol**
voltage in per unit	V_{pu}
rate of change of voltage	$\frac{dV}{dt}$
rate of change of real power	$\frac{dP}{dt}$
frequency	f
rate of change of frequency	$\frac{df}{dt}$
voltage total harmonic distortion	V_{THD}
current total harmonic distortion	I_{THD}

Table 6.2: Value of objective functions for single-source DG model

Events	**A**	**Se**	**Sp**	**P**
Capacitor Closing	99.96%	100%	99.96%	99.62%
Capacitor Opening	99.88%	100%	99.87%	99.77%
Line to Line Fault	100%	100%	100%	100%
Load Closing	99.90%	99%	99.99%	99.9%
Load Opening	99.88%	99.5%	99.92%	99.26%
Loss of Parallel Feeder	99.93%	100%	99.92%	99.26%
Reactive Mismatch (islanding)	99.62%	97.5%	99.84%	98.5%
Real Mismatch (islanding)	99.53%	97.4%	99.73%	99.55%
SLG Fault	99.98%	100%	99.98%	99.80%
Three Phase Fault	99.85%	98.4%	100%	100%
Normal Operation	99.80%	99.1%	99.87%	98.76%
Overall	**99.85%**	**99.17%**	**99.92%**	**99.22%**

islanding cases, and normal operation mode were considered in three classes, and values of the objective function from the confusion matrix were determined as recorded in Table 6.3. The high sensitivity of 99.4% indicates that the model did get confused between some real and reactive power mismatch cases. Furthermore, a high precision of 99.85% is proof that the proposed model can perform reliably in identifying the true negatives while predicting an islanding case. Overall high specificity values, as recorded in Table 6.3, also validate the robustness of this proposed classification technique.

Table 6.3: Value of objective functions for single-source DG model considering three classes

Events	**A**	**Se**	**Sp**	**P**
Non-islanding Cases	99.66%	99.8%	99.30%	99.74%
Islanding Cases	99.86%	99.40%	99.97%	99.85%
Normal operation	99.80%	99.1%	99.87%	98.76%
Overall	**99.73%**	**99.43%**	**99.71%**	**99.45%**

6.2 VALIDATION OF PROPOSED CLASSIFICATION TECHNIQUE

To validate the performance of the proposed classification technique, three cases were considered: 1) effect of noise in the dataset, 2) effect of multiple DG resources in the model, and 3) effect motor starting at both low voltage (LV) and high voltage (HV) side of the DG model.

6.2.1 EFFECT OF NOISE

As a validation of the efficiency of the proposed technique, the trained networks of all cross-validation cases were saved and tested with a 1050 new dataset with added white

Gaussian noise (AWGN) at 0, 10, 20, and 30 dB. The average classification accuracy of these datasets was listed in Table 6.4. The results indicate that the presence of noise in the signal data did not affect the performance of this proposed classification model.

Table 6.4: Prediction accuracy on normal and noisy unseen test data

AWGN Level	0	10 dB	20 dB	30 dB
Average Prediction Accuracy	99.35%	99.34%	99.34%	99.35%

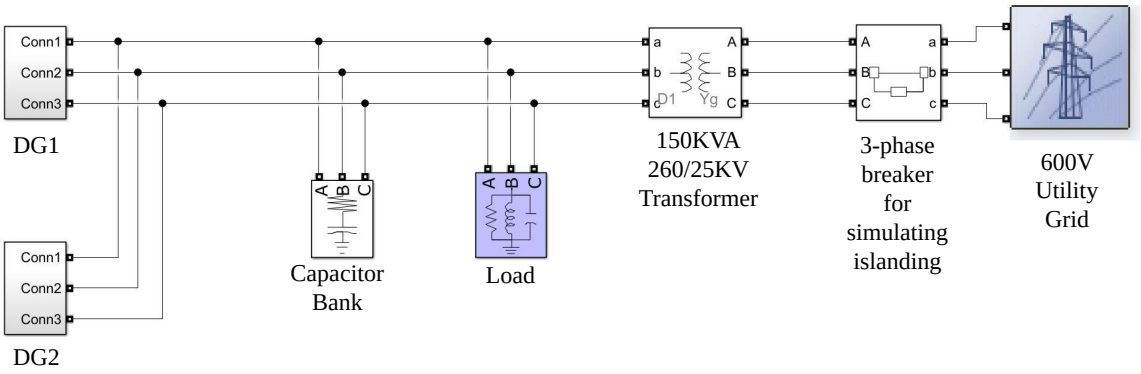

Figure 6.1: The Simulation model of a grid-connected PV system with two DG sources

6.2.2 Effect of Multiple DGs

The effects of the presence of multiple DG sources on the classification accuracy have also been investigated. A DG model with two 100 kW DG sources connected with the grid was considered, as shown in Fig. 6.1, and a total of 550 DG events mentioned earlier were simulated. Since the distribution transformer KVA rating had to be increased due to a change in maximum load from 100 kW to 200 kW, the trained classifier with the dataset of a single DG source model could not be used to make a prediction on the new data. This is because of the variations in the voltage signal during islanding as transformer impedance got changed (Guha, Haddad, and Kalaani 2016). So before training the classifier with a new

Table 6.5: Value of objective functions for multiple source DG model

Events	**A**	**Se**	**Sp**	**P**
Capacitor Closing	99.94%	99.4%	100%	100%
Capacitor Opening	99.96%	100%	99.96%	99.67%
Line to Line Fault	99.76%	98%	99.93%	99.45%
Load Closing	99.96%	99.6%	100%	100%
Load Opening	99.98%	100%	99.98%	99.81%
Loss of Parallel Feeder	99.89%	100%	99.88%	98.99%
Reactive Mismatch (islaning)	99.19%	95%	99.62%	96.52%
Real Mismatch (islaning)	99.19%	96.2%	99.49%	95.52%
SLG Fault	99.92%	100%	99.92%	99.43%
Three Phase Fault	99.80%	98.8%	99.90%	99.15%
Normal Operation	99.67%	98.2%	99.82%	98.5%
Overall	**99.75%**	**98.65%**	**99.86%**	**99%**

dataset, the optimum number of hidden units, maximum epoch, and mini-batch size were determined using GA as 86, 88, and 22, respectively. A similar process of 5-fold cross-validation was repeated for evaluating the classifier's performance with new input data. The classifier was able to classify the new data with an average classification accuracy of 98.65%. The average objective function values on each event are listed in Table 6.5

From the thorough investigation of the confusion matrix on each cross-validation case, it has been seen that none of the non-islanding cases were misclassified as an islanding case or vice-versa. The overall accuracy and specificity were almost the same as before. However, real power mismatch events, in some cases, were predicted as a reactive mismatch, which led to a reduction in the sensitivity and precision value of these two events. But still, all of the events were classified with a high overall sensitivity of 98.65% and overall precision of 98.82%. To justify this statement, the average value of the objective functions were determined considering all non-islanding events as one class, islanding cases as one class, and normal operation mode as a separate class, as stated in Table 6.6. The 100% overall accuracy, 100% sensitivity, 100% specificity, and 100% precision, indicate that the proposed classification technique is reliable for islanding detection even if there are more than one DG sources in the system.

Table 6.6: Value of objective functions for multiple source DG model considering three classes

Events	**A**	**Se**	**Sp**	**P**
Non-islanding Cases	99.67%	99.77%	99.40%	99.78%
Islanding Cases	100%	100%	100%	100%
Normal operation	99.67%	98.20%	99.82%	99.50%
Overall	**99.78%**	**99.32%**	**99.74%**	**99.76%**

6.2.3 Effect of Motor Starting Event

Finally, the effect of starting a large motor on both high voltage (HV) side and low voltage (LV) side on the classification accuracy was also investigated. The voltage of the system can fluctuate due to sudden motor starting events, which can be misclassified as islanding sometimes. Two cases were considered: the system model with a single DG source and multiple DG sources. Since, in both cases, the total number of events to be classified was changed into 13, the number fully connected layer was 13. So, new feature data of a motor starting in both cases were generated for a range of 10kVA- 300KVA nominal power rating on the HV side and 1 KVA- 30KVA nominal power rating on the LV side. These data were merged with the previous dataset, and the performance of the classification model was cross-validated. The average classification accuracy of the model with the motor starting event with a single DG source was 98.51%, while the average classification accuracy of the model with the motor starting event with multiple DG sources model was 98.42%. The accuracy, sensitivity, specificity, and precision of each event for both cases are listed in Table 6.7 and 6.8, which indicate that the proposed classification technique can make the DG model immune enough to avoid any false tripping due to the event like motor-starting.

Table 6.7: Effect of motor starting on the value of objective functions for single-source DG model

Events	**A**	**Se**	**Sp**	**P**
Capacitor Closing	99.91%	100%	99.92%	99.09%
Capacitor Opening	99.88%	99.8%	99.88%	99.75%
Line to Line Fault	99.78%	97.8%	99.95%	99.48%
Load Closing	99.91%	99.6%	99.93%	99.23%
Load Opening	99.76%	98.2%	99.89%	99.90%
Loss of Parallel Feeder	99.89%	100%	99.88%	98.76%
Reactive Mismatch (islanding)	99.53%	97.6%	99.70%	96.80%
Real Mismatch (islanding)	99.44%	95.2%	99.80%	99.84%
SLG Fault	100%	100%	100%	100%
Three Phase Fault	99.77%	98.4%	99.81%	98.73%
Normal Operation	99.46%	97.6%	99.61%	95.79%
Motor Starting at HV side	99.78%	98%	99.93%	99.30%
Motor Starting at LV side	99.85%	98.4%	99.98%	98.82%
Overall	**99.76%**	**98.56%**	**99.86%**	**98.73%**

Table 6.8: Effect of motor starting on the value of objective functions for multiple source DG model

Events	**A**	**Se**	**Sp**	**P**
Capacitor Closing	99.94%	99.8%	99.95%	99.48%
Capacitor Opening	99.98%	99.8%	100%	98.57%
Line to Line Fault	99.68%	97.6%	99.86%	98.58%
Load Closing	99.98%	100%	99.98%	99.82%
Load Opening	99.92%	99.6%	99.95%	99.48%
Loss of Parallel Feeder	99.81%	99.6%	99.83%	98.18%
Reactive Mismatch (islanding)	99.31%	95%	99.68%	96.53%
Real Mismatch (islanding)	99.32%	96.2%	99.58%	95.79%
SLG Fault	99.95%	100%	99.95%	99.46%
Three Phase Fault	99.81%	98.4%	99.93%	98.3%
Normal Operation	99.58%	96.6%	99.83%	98.12%
Motor Starting at HV side	99.75%	97.8%	99.92%	99.09%
Motor Starting at LV side	99.73%	99%	99.80%	97.8%
Overall	**99.76%**	**98.42%**	**99.87%**	**98.61%**

CHAPTER 7

CONCLUSION

A proper classification technique in a distributed generation system can improve the fault identification system and prevent false triggers of a non-islanding event as an islanding event or vice-versa. Many studies have investigated different classification techniques to classify islanding and non-islanding cases. However, most of them were unable to classify these events to their root cause. Moreover, the normal operation mode was not included in those classification techniques, which can be an essential factor since many of the non-islanding or islanding cases can be misjudged by normal operation mode by the existing protective system.

The proposed event classification technique based on RNN using LSTM has performed adequately in all cases mentioned above with high overall accuracy, sensitivity, specificity, and precision. Since traditional LSTM suffers from poorly chosen values of training parameters for the dataset with temporal patterns, GA has been integrated into the LSTM model to search for optimized model parameters and input features. Classification accuracy, as well as overall performance, has been improved significantly with the optimal combination of features selected by GA. Non-islanding cases and islanding cases, including normal operation mode, have been classified with an average classification accuracy of 99.17% for the DG model having a single DG source.

As a verification of the effectiveness and robustness of the technique, the model's performance has been evaluated for large datasets in a standard and noisy environment, presence of multiple DG sources, and the inclusion of motor starting event in the dataset. The trained model's prediction accuracy was as high as 99.34%, 99.34%, 99.35%, with noisy test data at 10dB, 20 dB, and 30 dB. The ability of the proposed model to predict noisy time-series patterns can be useful in many domains. The overall performance of this technique remained unaffected after the inclusion of multiple DGs or motor starting events.

The average classification accuracy of the model with multiple DG sources was 98.65%. Finally, we suggest a classification technique that does not require any pre-processing of extracted time-series signals and have less restriction. The GA optimized technique based on RNN using LSTM can be applied in domains like biomedical, health science, stock-exchange, and weather forecasting effectively.

REFERENCES

Agency, United States Environmental Protection. 2018. *Distributed Generation of Electricity and its Environmental Impacts.* Accessed March 13, 2018. https://www.epa.gov/energy/distributed-generation-electricity-and-its-environmental-impacts.

Ahmadipour, M., G. Borbad M., and H. Hizam. 2019. "A New Islanding Detection Scheme Based on Combination of Slantlet Transform and Probabilistic Neural Network for Grid-Tied Photovoltaic System." In *2019 International Youth Conference on Radio Electronics, Electrical and Power Engineering (REEPE),* 1–6. doi:10.1109/REEPE.2019.8708802.

Ahmadipour, M., H. Hizam, M. L. Othman, and M. A. Radzi. 2019. "Islanding detection method using ridgelet probabilistic neural network in distributed generation." *Neurocomputing* 329:188–209.

Akhlaghi, S., A. A. Ghadimi, and A. Akhlaghi. 2014. "A novel hybrid islanding detection method combination of SMS and Q-f for islanding detection of inverter- based DG." in *2014 Power and Energy Conference at Illinois (PECI).*

Alam, M. R., K. M. Muttaqi, and A. Bouzerdoum. 2014. "An Approach for Assessing the Effectiveness of Multiple-Feature-Based SVM Method for Islanding Detection of Distributed Generation." *IEEE Transactions on Industry Applications* 50 (4): 2844–2852.

Arritt, R. F., and R. C. Dugan. 2015. "Review of the Impacts of Distributed Generation on Distribution Protection." In *2015 IEEE Rural Electric Power Conference,* 69–74. doi:10.1109/REPC.2015.12.

Asiminoaei, L., R. Teodorescu, F. Blaabjerg, and U. Borup. 2005. "A digital controlled PV-inverter with grid impedance estimation for ENS detection." *IEEE Transactions on Power Electronics* 20 (6): 1480–1490.

Azim, R., F. Li, Y. Xue, M. Starke, and H. Wang. 2017. "An islanding detection methodology combining decision trees and Sandia frequency shift for inverter-based distributed generations." *IET Generation, Transmission Distribution* 11 (16): 4104–4113. doi:10.1049/iet-gtd.2016.1617.

Baghaee, H. R., D. Mlakić, S. Nikolovski, and T. Dragičević. 2019a. "Anti-Islanding Protection of PV-based Microgrids Consisting of PHEVs using SVMs." *IEEE Transactions on Smart Grid:* 1–1.

———. 2019b. "Support vector machine-based Islanding and grid fault detection in active distribution networks." *IEEE Journal of Emerging and Selected Topics in Power Electronics.*

Bari, N. A., and S. D. Jawale. 2016. "Smart and adaptive protection scheme for distribution network with distributed generation: A scoping review." In *2016 International Conference on Energy Efficient Technologies for Sustainability (ICEETS),* 569–572. doi:10.1109/ICEETS.2016.7583818.

Basak, P., S. Chowdhury, S. Halder nee Dey, and S.P. Chowdhury. 2012. "A literature review on integration of distributed energy resources in the perspective of control, protection and stability of microgrid." *Renewable and Sustainable Energy Reviews* 16 (8): 5545–5556.

Bengio, Y., N. Boulanger-Lewandowski, and R. Pascanu. 2013. "Advances in optimizing recurrent networks." In *2013 IEEE International Conference on Acoustics, Speech and Signal Processing,* 8624–8628.

Bishop, Christopher M. 2006. *Pattern Recognition and Machine Learning (Information Science and Statistics).* Berlin, Heidelberg: Springer-Verlag.

Boehme, T., G. P. Harrison, and A. R. Wallace. 2010. "Assessment of distribution network limits for non-firm connection of renewable generation." *IET Renewable Power Generation* 4 (1): 64–74.

Chad, A., Y. Brissette, and V. Philippe. 2014. "An Autoground System for Anti-Islanding Protection of Distributed Generation." *Power Systems, IEEE Transactions on* 29 (March): 873–880. doi:10.1109/TPWRS.2013.2284670.

Chakravorti, T., R. K. Patnaik, and P. K. Dash. 2018. "Detection and classification of islanding and power quality disturbances in microgrid using hybrid signal processing and data mining techniques." *IET Signal Processing* 12 (1): 82–94. doi:10.1049/iet-spr.2016.0352.

Chandak, S., M. Mishra, S. Nayak, and P. K. Rout. 2018. "Optimal feature selection for islanding detection in distributed generation." *IET Smart Grid* 1 (3): 85–95. doi:10.1049/iet-stg.2018.0021.

Chen, X., and Y. Li. 2016. "An Islanding Detection Method for Inverter-Based Distributed Generators Based on the Reactive Power Disturbance." *IEEE Transactions on Power Electronics* 31 (5): 3559–3574.

Chen, X., X. Wang, J. Jian, Z. Tan, Y. Li, and P. Crossley. 2019. "Novel islanding detection method for inverter-based distributed generators based on adaptive reactive power control." *The Journal of Engineering* 2019 (17): 3890–3894(4).

Das, P. P., and S. Chattopadhyay. 2018. "A Voltage-Independent Islanding Detection Method and Low-Voltage Ride Through of a Two-Stage PV Inverter." *IEEE Transactions on Industry Applications* 54 (3): 2773–2783. doi:10.1109/TIA.2017.2788433.

Dubey, R., M. Popov, and S. R. Samantaray. 2019. "Transient monitoring function-based islanding detection in power distribution network." *IET Generation, Transmission Distribution* 13 (6): 805–813.

Eristi, Huseyin, Ozal Yildirim, Belkis Eiristi, and Yakup Demir. 2013. "Optimal feature selection for classification of the power quality events using wavelet transform and least squares support vector machines." *International Journal of Electrical Power & Energy Systems* 49:95–103.

EURELECTRIC. 2013. "Active Distribution System Management: A Key Tool For The Smooth Integration Of Distributed Generation."

Farhan, M. A., and S. S. K. 2017. "Mathematical morphology-based islanding detection for distributed generation." *IET Generation, Transmission Distribution* 11 (14): 3449–3457. doi:10.1049/iet-gtd.2016.1163.

Feng, J., B. Zeng, D. Zhao, G. Wu, Z. Liu, and J. Zhang. 2018. "Evaluating Demand Response Impacts on Capacity Credit of Renewable Distributed Generation in Smart Distribution Systems." *IEEE Access* 6:14307–14317.

Ganivada, P. K., and P. Jena. 2019. "Passive Islanding Detection Techniques Using Synchrophasors for Inverter Based Distributed Generators." In *2019 IEEE PES GTD Grand International Conference and Exposition Asia (GTD Asia),* 747–751.

Gao, S., K. Wang, and B. Yun. 2019. "A new islanding detection method for grid-connected photovoltaic system based on harmonic impedance sequence component." *IET Conference Proceedings:* 60 (5 pp.)–60 (5 pp.)(1).

Georgilakis, P. S., and N. D. Hatziargyriou. 2013. "Optimal Distributed Generation Placement in Power Distribution Networks: Models, Methods, and Future Research." *IEEE Transactions on Power Systems* 28 (3): 3420–3428. doi:10.1109/TPWRS.2012.2237043.

Giroux, P., G. Sybille, C. Osorio, and S. Chandrachood. n.d. "Average Model of a 100-kW Grid-Connected PV Array." https://www.mathworks.com/help/physmod/sps/examples/average-model-of-a-100-kw-grid-connected-pv-array.html.

Guha, B., R. J. Haddad, and Y. Kalaani. 2015a. "A novel passive islanding detection technique for converter-based distributed generation systems." In *2015 IEEE Power Energy Society Innovative Smart Grid Technologies Conference (ISGT),* 1–5. doi:10.1109/ISGT.2015.7131907.

———. 2015b. "A passive islanding detection approach for inverter-based distributed generation using rate of change of frequency analysis." In *SoutheastCon 2015,* 1–6.

———. 2015c. "Anti-islanding techniques for Inverter-based Distributed Generation systems - A survey." In *SoutheastCon 2015,* 1–9. doi:10.1109/SECON.2015.7133045.

———. 2016. "Voltage Ripple-Based Passive Islanding Detection Technique for Grid-Connected Photovoltaic Inverters." *IEEE Power and Energy Technology Systems Journal* 3 (4): 143–154. doi:10.1109/JPETS.2016.2586847.

Gupta, P., R. S. Bhatia, and D. K. Jain. 2015. "Average Absolute Frequency Deviation Value Based Active Islanding Detection Technique." *IEEE Transactions on Smart Grid* 6 (1): 26–35.

Haddad, R. J., B. Guha, Y. Kalaani, and A. El-Shahat. 2018. "Smart Distributed Generation Systems Using Artificial Neural Network-Based Event Classification." *IEEE Power and Energy Technology Systems Journal* 5 (2): 18–26. doi:10.1109/JPETS.2018.2805894.

Haoran, C., X. Jianyuan, L. Hui, C. Guoqiang, J. Yuanyu, C. Shengwei, and C. Jiangbo. 2019. "Islanding detection method of distribution generation system based on logistic

regression." *The Journal of Engineering* 2019 (16): 2296–2300. doi:10.1049/joe.2018.8794.

Hasan, A. M. 2019. "A Modified Incremental Conductance Based Photovoltaic MPPT Charge Controller." February. doi:10.1109/ECACE.2019.8679308.

Hochreiter, S. 1991. "Untersuchungen zu dynamischen neuronalen Netzen." *Diploma, Technische Universität München* 91 (1).

Hopfield, J J. 1982. "Neural networks and physical systems with emergent collective computational abilities." *Proceedings of the National Academy of Sciences* 79 (8): 2554–2558. doi:10.1073/pnas.79.8.2554.

Hsieh, Cheng-Tao, Jeu-Min Lin, and Shyh-Jier Huang. 2008. "Enhancement of islanding-detection of distributed generation systems via wavelet transform-based approaches." *International Journal of Electrical Power & Energy Systems* 30 (10): 575–580.

IEC62116. 2008. "International standard, test procedure for utility-interconnected photovoltaic inverters."

IEEE1547. 2003. "IEEE Standard for Interconnecting Distributed Resources with Electric Power Systems." *IEEE Std 1547-2003:* 1–28.

Järventausta, Pertti, Sami Repo, Antti Rautiainen, and Jarmo Partanen. 2010. "Smart grid power system control in distributed generation environment." *Annual Reviews in Control* 34 (2): 277–286.

Jinsong, T., H. Haihong, W. Zhe, S. Yang, F. Wei, and L. Yong. 2018. "An Advanced Islanding Detection Strategy Coordinating the Newly Proposed V Detection and the ROCOF Detection," 1204–1208. May. doi:10.1109/ISGT-Asia.2018.8467902.

Keane, A., L. F. Ochoa, C. L. T. Borges, G. W. Ault, A. D. Alarcon-Rodriguez, R. A. F. Currie, F. Pilo, C. Dent, and G. P. Harrison. 2013. "State-of-the-Art Techniques and Challenges Ahead for Distributed Generation Planning and Optimization." *IEEE Transactions on Power Systems* 28 (2): 1493–1502.

Kermany, S. D., M. Joorabian, S. Deilami, and M. A. S. Masoum. 2017. "Hybrid Islanding Detection in Microgrid With Multiple Connection Points to Smart Grids Using Fuzzy-Neural Network." *IEEE Transactions on Power Systems* 32 (4): 2640–2651.

Khamis, A., H. Shareef, E. Bizkevelci, and T. Khatib. 2013. "A review of islanding detection techniques for renewable distributed generation systems." *Renewable and Sustainable Energy Reviews* 28:483–493. doi:https://doi.org/10.1016/j.rser.2013.08.025.

Khodaparastan, M., H. Vahedi, F. Khazaeli, and H. Oraee. 2017. "A Novel Hybrid Islanding Detection Method for Inverter-Based DGs Using SFS and ROCOF." *IEEE Transactions on Power Delivery* 32 (5): 2162–2170.

Khokhar, Suhail, Abdullah Asuhaimi Mohd Zin, Aslam Pervez Memon, and Ahmad Safawi Mokhtar. 2017. "A new optimal feature selection algorithm for classification of power quality disturbances using discrete wavelet transform and probabilistic neural network." *Measurement* 95:246–259.

Kim, D., and S. Kim. 2019. "Anti-Islanding Detection Method Using Phase-Shifted Feed-Forward Voltage in Grid-Connected Inverter." *IEEE Access* 7:147179–147190.

Kong, X., X. Xu, Z. Yan, S. Chen, H. Yang, and D. Han. 2018. "Deep learning hybrid method for islanding detection in distributed generation." *Applied Energy* 210:776–785.

Kumar, D., and P. S. Bhowmik. 2018. "Artificial neural network and phasor data-based islanding detection in smart grid." *IET Generation, Transmission Distribution* 12 (21): 5843–5850. doi:10.1049/iet-gtd.2018.6299.

Laghari, J. A., H. Mokhlis, M. Karimi, A. H. A. Bakar, and A. Shahriari. 2014. "Artificial neural network based islanding detection technique for mini hydro type distributed generation." In *3rd IET International Conference on Clean Energy and Technology (CEAT) 2014,* 1–6.

Li, Y., P. Zhang, W. Li, J. N. Debs, D. A. Ferrante, D. J. Kane, S. N. Woolard, R. Kalbfleisch, K. B. Bowes, and A. J. Kasznay. 2019. "Nondetection Zone Analytics for Unintentional Islanding in a Distribution Grid Integrated With Distributed Energy Resources." *IEEE Transactions on Sustainable Energy* 10 (1): 214–225. doi:10.1109/TSTE.2018.2830748.

Madani, S. S., A. Abbaspour, M. Beiraghi, P. Z. Dehkordi, and A. M. Ranjbar. 2012. "Islanding detection for PV and DFIG using decision tree and AdaBoost algorithm." In *2012 3rd IEEE PES Innovative Smart Grid Technologies Europe (ISGT Europe),* 1–8.

Makwana, Y. M., and B. R. Bhalja. 2017. "Islanding detection technique based on superimposed components of voltage." *IET Renewable Power Generation* 11 (11): 1371–1381.

———. 2019. "Experimental Performance of an Islanding Detection Scheme Based on Modal Components." *IEEE Transactions on Smart Grid* 10 (1): 1025–1035.

Makwana, Y. M., B. R. Bhalja, and R. Gokaraju. 2019. "Auto-correlation-based Islanding detection technique verified through hardware-in-loop testing." *IET Generation, Transmission Distribution* 13 (17): 3792–3802.

Makwana, Y., and B. R. Bhalja. 2016. "Islanding detection technique based on relevance vector machine." *IET Renewable Power Generation* 10 (10): 1607–1615.

Manikonda, S. K. G., and D. N. Gaonkar. 2019. "IDM based on image classification with CNN." *The Journal of Engineering* 2019 (10): 7256–7262. doi:10.1049/joe.2019.0025.

Matic-Cuka, B., and M. Kezunovic. 2014. "Islanding detection for inverter-based distributed generation using support vector machine method." *IEEE Transactions on Smart Grid* 5 (6): 2676–2686.

McCulloch, Warren S., and P. Walter. 1943. "A logical calculus of the ideas immanent in nervous activity." *The bulletin of mathematical biophysics* 5 (4): 115–133.

Mehang, T. S., D. C. Riawan, and V. L. B. Putri. 2018. "Islanding Detection in Grid-Connected Distributed Photovoltaic Generation Using Artificial Neural Network." In *2018 International Seminar on Intelligent Technology and Its Applications (ISITIA),* 181–186.

Menezes, T. S., P. I. N. Barbalho, D. V. Coury, and R. A. S. Fernandes. 2019. "Islanding Detection for Distributed Generators Based on Artificial Neural Network and S-transform." In *2019 IEEE PES Innovative Smart Grid Technologies Conference - Latin America (ISGT Latin America),* 1–5.

Menezes, T. S., D. V. Coury, and R. A. S. Fernandes. 2019. "Islanding Detection Based on Artificial Neural Network and S-transform for Distributed Generators." In *2019 IEEE Milan PowerTech,* 1–6.

Mishra, M., R. R. Panigrahi, and P. K. Rout. 2019. "A combined mathematical morphology and extreme learning machine techniques based approach to micro-grid protection." *Ain Shams Engineering Journal* 10 (2): 307–318.

Mishra, M., and P. K. Rout. 2018. "Detection and classification of micro-grid faults based on HHT and machine learning techniques." *IET Generation, Transmission Distribution* 12 (2): 388–397. doi:10.1049/iet-gtd.2017.0502.

Mlakic, D., H. R. Baghaee, and S. Nikolovski. 2019a. "A Novel ANFIS-Based Islanding Detection for Inverter-Interfaced Microgrids." *IEEE Transactions on Smart Grid* 10 (4): 4411–4424.

———. 2019b. "Gibbs Phenomenon-Based Hybrid Islanding Detection Strategy for VSC-Based Microgrids Using Frequency Shift, THD_U , and RMS_U." *IEEE Transactions on Smart Grid* 10 (5): 5479–5491.

Mohanty, S. R., N. Kishor, R. S. H., and A. T. K. 2019. "Real-Time Implementation of Signal Processing Techniques for Disturbances Detection." *IEEE Transactions on Industrial Electronics* 66 (5): 3550–3560. doi:10.1109/TIE.2018.2851968.

Muda, H., and P. Jena. 2018. "Phase angle-based PC technique for islanding detection of distributed generations." *IET Renewable Power Generation* 12 (6): 735–746.

Murugesan, S., and V. Murali. 2019a. "Band pass filter and AFVmean-based unintentional islanding detection." *IET Generation, Transmission & Distribution* 13 (9): 1489–1498(9).

———. 2019b. "Hybrid Analyzing Technique Based Active Islanding Detection for Multiple DGs." *IEEE Transactions on Industrial Informatics* 15 (3): 1311–1320.

Murugesan, S., V. Murali, and S. A. Daniel. 2018. "Hybrid Analyzing Technique for Active Islanding Detection Based on d-Axis Current Injection." *IEEE Systems Journal* 12 (4): 3608–3617. doi:10.1109/JSYST.2017.2730364.

Niaki, A.H. Mohammadzadeh, and S. Afsharnia. 2014. "A new passive islanding detection method and its performance evaluation for multi-DG systems." *Electric Power Sys-*

tems Research 110:180–187. doi:https://doi.org/10.1016/j.epsr.2014.01.016. http://www.sciencedirect.com/science/article/pii/S0378779614000200.

Olah, C. 2015. *Understanding LSTM Networks.* https://colah.github.io/posts/2015-08-Understanding-LSTMs/.

OpenEi. 2018. "Distributed Generation." https://openei.org/wiki/Distributed_Generation.

Park, S., M. Kwon, and S. Choi. 2019. "Reactive Power P O Anti-Islanding Method for a Grid-Connected Inverter With Critical Load." *IEEE Transactions on Power Electronics* 34 (1): 204–212.

Pena, P., A. Etxegarai, L. Valverde, I. Zamora, and R. Cimadevilla. 2013. "Synchrophasor-based anti-islanding detection." In *2013 IEEE Grenoble Conference,* 1–6.

Ray, P. K., N. Kishor, and S. R. Mohanty. 2010. "S-transform based islanding detection in grid-connected distributed generation based power system." In *2010 IEEE International Energy Conference,* 612–617.

Ray, P. K., S. R. Mohanty, and N. Kishor. 2013. "Classification of Power Quality Disturbances Due to Environmental Characteristics in Distributed Generation System." *IEEE Transactions on Sustainable Energy* 4 (2): 302–313. doi:10.1109/TSTE.2012.2224678.

Raza, S., H. Arof, H. Mokhlis, H. Mohamad, and H. A. Illias. 2017. "Passive islanding detection technique for synchronous generators based on performance ranking of different passive parameters." *IET Generation, Transmission Distribution* 11 (17): 4175–4183.

Reigosa, D. D., F. Briz, C. Blanco Charro, and J. M. Guerrero. 2017. "Passive Islanding Detection Using Inverter Nonlinear Effects." *IEEE Transactions on Power Electronics* 32 (11): 8434–8445.

Robinson, A. J., and Frank Fallside. 1987. *The Utility Driven Dynamic Error Propagation Network.* Technical report CUED/F-INFENG/TR.1. Cambridge, UK: Engineering Department, Cambridge University.

Ropp, M. E., K. Aaker, J. Haigh, and N. Sabbah. 2000. "Using power line carrier communications to prevent islanding of PV power systems." In *Conference Record of the Twenty-Eighth IEEE Photovoltaic Specialists Conference - 2000 (Cat. No.00CH37036),* 1675–1678.

Ropp, M. E., M. Begovic, and A. Rohatgi. 1999. "Analysis and performance assessment of the active frequency drift method of islanding prevention." *IEEE Transactions on Energy Conversion* 14 (3): 810–816.

Rostami, A., A. Jalilian, M. T. Hagh, K. M. Muttaqi, and J. Olamaei. 2019. "Islanding Detection of Distributed Generation Based on Rate of Change of Exciter Voltage With Circuit Breaker Switching Strategy." *IEEE Transactions on Industry Applications* 55 (1): 954–963.

Ruchita, N., V. Kasimala, B. Sandeep, B. Monalisa, and K. Nand. 2018. "Islanding Detection in Distributed Generation System using Intrinsic Time Decomposition." *IET Generation, Transmission and Distribution* 13 (November). doi:10.1049/iet-gtd.2018.5645.

Saleh, S. A., A. S. Aljankawey, R. Meng, J. Meng, L. Chang, and C. P. Diduch. 2016. "Apparent Power-Based Anti-Islanding Protection for Distributed Cogeneration Systems." *IEEE Transactions on Industry Applications* 52 (1): 83–98.

Samui, A., and S. R. Samantaray. 2013. "Wavelet Singular Entropy-Based Islanding Detection in Distributed Generation." *IEEE Transactions on Power Delivery* 28 (1): 411–418. doi:10.1109/TPWRD.2012.2220987.

Santoso, S., W. M. Grady, E. J. Powers, J. Lamoree, and S. C. Bhatt. 2000. "Characterization of distribution power quality events with Fourier and wavelet transforms." *IEEE Transactions on Power Delivery* 15 (1): 247–254. doi:10.1109/61.847259.

Sepp, H., and S. Jürgen. 1997. "Long Short-Term Memory." *Neural Comput.* (Cambridge, MA, USA) 9 (8): 1735–1780.

Siddiqui, S. A., M. Fozdar, and N. K. 2017. "Hybrid islanding detection method and priority-based load shedding for distribution networks in the presence of DG units." *IET Generation, Transmission Distribution* 11 (3): 586–595.

Stone, M. 1974. "Cross-Validatory Choice and Assessment of Statistical Predictions." *Journal of the Royal Statistical Society. Series B (Methodological)* 36 (2): 111–147.

Sun, Q., J. M. Guerrero, T. Jing, J. C. Vasquez, and R. Yang. 2017. "An Islanding Detection Method by Using Frequency Positive Feedback Based on FLL for Single-Phase Microgrid." *IEEE Transactions on Smart Grid* 8 (4): 1821–1830.

Sun, R., Z. Wu, and V. A. Centeno. 2011. "Power system islanding detection identification using topology approach and decision tree." In *2011 IEEE Power and Energy Society General Meeting,* 1–6.

Sykes, J., K. Koellner, W. Premerlani, B. Kasztenny, and M. Adamiak. 2007. "Synchrophasors: A primer and practical applications." In *2007 Power Systems Conference: Advanced Metering, Protection, Control, Communication, and Distributed Resources,* 213–240.

Tom, F. 2006. "An Introduction to ROC Analysis." *Pattern Recogn. Lett.* (New York, NY, USA) 27 (8): 861–874.

UL1741. 2001. "UL1741 Standard for Inverters, Converters, Controllers and Interconnection System Equipment for Use With Distributed Energy Resources."

Vahedi, H., G. B. Gharehpetian, and M. Karrari. 2012. "Application of Duffing Oscillators for Passive Islanding Detection of Inverter-Based Distributed Generation Units." *IEEE Transactions on Power Delivery* 27 (4): 1973–1983. doi:10.1109/TPWRD.2012.2212251.

Vahedi, H., and M. Karrari. 2013. "Adaptive Fuzzy Sandia Frequency-Shift Method for Islanding Protection of Inverter-Based Distributed Generation." *IEEE Transactions on Power Delivery* 28 (1): 84–92.

Voglitsis, D., N. P. Papanikolaou, and A. C. Kyritsis. 2019. "Active Cross-Correlation Anti-Islanding Scheme for PV Module-Integrated Converters in the Prospect of High Penetration Levels and Weak Grid Conditions." *IEEE Transactions on Power Electronics* 34 (3): 2258–2274.

Wang, W., J. Kliber, G. Zhang, W. Xu, B. Howell, and T. Palladino. 2007. "A Power Line Signaling Based Scheme for Anti-Islanding Protection of Distributed Generators—Part II: Field Test Results." *IEEE Transactions on Power Delivery* 22 (3): 1767–1772.

Wang, Y., J. Ravishankar, and T. Phung. 2019. "Wavelet transform-based feature extraction for detection and classification of disturbances in an islanded micro-grid." *IET Generation, Transmission Distribution* 13 (11): 2077–2087.

Ward, B., and R. Michael. 2002. "Evaluation of Islanding Detection Methods for Utility-Interactive Inverters in Photovoltaic Systems" (January). doi:10.2172/806700.

Wen, B., D. Boroyevich, R. Burgos, Z. Shen, and P. Mattavelli. 2016. "Impedance-Based Analysis of Active Frequency Drift Islanding Detection for Grid-Tied Inverter System." *IEEE Transactions on Industry Applications* 52 (1): 332–341.

Werbos, Paul J. 1988. "Generalization of backpropagation with application to a recurrent gas market model." *Neural Networks* 1 (4): 339–356.

Williams, Ronald J., and David Zipser. 1995. *Gradient-Based Learning Algorithms for Recurrent Networks and Their Computational Complexity.*

Xu, W., G. Zhang, C. Li, W. Wang, G. Wang, and J. Kliber. 2007. "A Power Line Signaling Based Technique for Anti-Islanding Protection of Distributed Generators—Part I: Scheme and Analysis." *IEEE Transactions on Power Delivery* 22 (3): 1758–1766.

Yafaoui, A., B. Wu, and S. Kouro. 2012. "Improved Active Frequency Drift Anti-islanding Detection Method for Grid Connected Photovoltaic Systems." *IEEE Transactions on Power Electronics* 27 (5): 2367–2375.